TN-20
195463
50P

NASA TN D-66

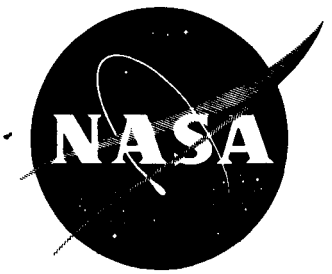

TECHNICAL NOTE

D-66

ANALYSIS OF EFFECTS OF ROCKET-ENGINE DESIGN PARAMETERS ON REGENERATIVE-COOLING CAPABILITIES OF SEVERAL PROPELLANTS

By Arthur N. Curren, Harold G. Price, Jr., and Howard W. Douglass

Lewis Research Center
Cleveland, Ohio

NATIONAL AERONAUTICS AND SPACE ADMINISTRATION

WASHINGTON September 1959

(NASA-TN-D-66) ANALYSIS OF EFFECTS OF ROCKET-ENGINE DESIGN PARAMETERS ON REGENERATIVE-COOLING CAPABILITIES OF SEVERAL PROPELLANTS (NASA. Lewis Research Center) 50 p

N89-70679

Unclas
00/20 0195463

NATIONAL AERONAUTICS AND SPACE ADMINISTRATION

TECHNICAL NOTE D-66

ANALYSIS OF EFFECTS OF ROCKET-ENGINE DESIGN PARAMETERS ON REGENERATIVE-COOLING CAPABILITIES OF SEVERAL PROPELLANTS

By Arthur N. Curren, Harold G. Price, Jr., and Howard W. Douglass

E-150

CJ-1

SUMMARY

An analytical study was conducted to determine the influence of several design parameters on the cooling requirements of some high-energy, regeneratively fuel-cooled rocket engines. These parameters include engine size, combustion-chamber pressure, contraction and expansion area ratios, propellant combination, fuel-oxidant mixture ratio, and performance efficiency. The nominal thrust levels considered were 1000, 10,000, 100,000, and 1,000,000 pounds; and the propellant combinations were hydrogen-fluorine (H_2-F_2), hydrogen-oxygen (H_2-O_2), hydrazine-fluorine (N_2H_4-F_2), ammonia-fluorine (NH_3-F_2), and jet-engine fuel and oxygen (JP4-O_2). The engines considered were of cylindrical chamber design, and expansion to sea-level conditions was specified except where variations in expansion area ratio were under study. The cooling system was such that the fuel flowed axially (from nozzle exit to injector) in an annular jacket along the entire engine length. Some of the engines employed the additional cooling aid of a ceramic lining in the combustion chamber and nozzle.

The analysis revealed the areas of feasible application of regenerative fuel-cooling for the various propellant combinations. In general, propellant combinations using hydrogen as the fuel and coolant displayed the best cooling possibilities of the combinations studied. The application of chamber and nozzle ceramic linings, of course, improves the possibility of cooling where it might otherwise be marginal or impossible. The most important influencing parameters with respect to the cooling requirement of a particular propellant combination, in approximate order of decreasing influence, are engine size, performance efficiency, fuel-oxidant mixture ratio, expansion area ratio, combustion-chamber pressure, and contraction area ratio.

E-150

INTRODUCTION

The fundamental problem in cooling a rocket engine is to devise a means of transferring heat from the combustion zone to some heat sink so that safe low structural temperatures may be maintained. In a regeneratively cooled engine, the heat sink is one or both of the incoming propellant components, directed in some manner along the combustion-chamber and nozzle outer surfaces. By this method, the inside, or combustion-gas side, of the engine walls is cooled so that its temperature does not rise high enough to permit melting, oxidation, or erosion failures, categorically classified as "burnouts." The amount of heat required to be transferred is a function of propellant combination, the relative amount of fuel in the mixture, combustion-chamber pressure, thrust level, and engine geometry, while the amount of heat the coolant is capable of absorbing is a function of the coolant properties, coolant flow rate, and the coolant jacket configuration. The interrelation of these variables must be known in order to design a regeneratively cooled rocket engine successfully. This interrelation is the subject of the present report.

To gain some insight into the interdependence of these variables, heat-transfer requirements were studied for engines using several propellant combinations, including hydrogen-fluorine (H_2-F_2), hydrogen-oxygen (H_2-O_2), hydrazine-fluorine (N_2H_4-F_2), ammonia-fluorine (NH_3-F_2), and jet-engine fuel and oxygen (JP4-O_2). Nominal thrust levels of 1000, 10,000, 100,000, and 1,000,000 pounds were assumed; and representative ranges of combustion-chamber pressures, fuel mixture ratios, performance efficiencies, and engine contraction and expansion area ratios were considered.

The potentialities of cooling augmentation by the use of ceramic coatings were also included.

METHOD OF ANALYSIS

Heat-Transfer Calculations

Combustion gas to engine walls. - Heat transfer from the hot combustion gases to the cooled combustion-chamber walls, which is mainly by convection, is the subject of much study today. Radiation effects and dissociation phenomena, too, certainly require much study, along with attending boundary-layer analysis, before any approach can be made to an "exact" heat-transfer solution. It is sufficient to say at this point, however, that no one unified and workable technique for evaluating heat transfer in this area is now available. Therefore, in order to proceed with the desired analysis, it was necessary to employ an approximation for the heat-transfer mechanism from combustion gas to engine walls. Reference 1 shows that the heat transfer associated with

a turbulent boundary layer can be approximated quite closely by a dimensionless number correlation for fully developed turbulent flow in pipes, even though fully developed turbulent flow is not necessarily assumed for the rocket engine.

The relation utilized in this study to describe the heat-transfer mechanism for this condition is a form of the dimensionless number correlation for fully developed turbulent flow in a tube suggested by reference 2:

$$Nu = 0.023(Re)^{0.8}(Pr)^{0.333} \tag{1}$$

(All symbols are defined in appendix A.) It should be noted that this relation does not deal specifically with effects of radiation and/or dissociation, other than those effects present in the experiments from which the coefficient and exponents were evaluated. Radiation heat transfer was estimated, on the basis of cursory calculations, to account for less than 5 percent of the total for the high-energy propellant combinations considered in this study. In more basic symbols, this equation is commonly written as follows:

$$\frac{h\bar{D}}{k} = 0.023\left(\frac{\rho u \bar{D}}{\mu}\right)^{0.8}\left(\frac{c_p \mu}{k}\right)^{0.333}$$

This correlation, as first proposed, based the physical properties of the fluid involved on the bulk, or free-stream temperature, with the exception of viscosity, which was based on the film temperature, or average of free-stream and wall temperatures. This temperature basis seems fairly obvious, since the correlation was developed for moderate heat fluxes and temperature levels, and the temperature profile along a tube diameter in that case would be relatively flat. However, with the heat flux and temperature levels encountered in a cooled rocket engine, rapidly changing diametral temperatures and fluid properties occur, particularly near the cooled walls. It would seem logical then that the physical properties of the combustion gas required in the use of equation (1) should be based on the film temperature at the cooled walls. This concept is of course well established, and discussions appear in references 2 and 3, as well as in many other studies. Use of this method to compute combustion-gas to engine-wall heat-transfer rates has exhibited reasonable agreement with experiments on cooled rocket engines. The film temperature referred to in this study is defined, as suggested earlier, by the relation

$$T_{g,f} = 0.5(T_{g,s} + T_{g,w}) \tag{2}$$

The evaluation of Reynolds number Re for use in equation (1) is not straightforward, since it involves density, a property not explicitly tabulated in the available literature. It has been found convenient to

perform a simple manipulation to expedite this determination. From continuity considerations, the following may be written:

$$\frac{w_p}{A_g} = G_g = \rho_{g,s} u_{g,s} = \rho_{g,f} \left(\frac{\rho_{g,s}}{\rho_{g,f}} \right) u_{g,s} \tag{3}$$

From the perfect gas relation, the density ratio $\rho_{g,s}/\rho_{g,f}$ may be written as

$$\frac{\rho_{g,s}}{\rho_{g,f}} = \frac{p_{g,s} R_{g,f} T_{g,f}}{p_{g,f} R_{g,s} T_{g,s}}$$

Using the common assumption that the static pressure through a turbulent boundary layer remains constant (ref. 4), and further assuming that the change in molecular weight of the fluid is insignificantly small, equation (3) can be rewritten as

$$G_g = \rho_{g,f} \left(\frac{T_{g,f}}{T_{g,s}} \right) u_{g,s}$$

The Reynolds number may now be written in terms of explicitly defined values, and equation (1) becomes

$$\frac{h_{g,f} \bar{D}_g}{k_{g,f}} = 0.023 \left(\frac{G_g \bar{D}_g}{\mu_{g,f}} \cdot \frac{T_{g,s}}{T_{g,f}} \right)^{0.8} \left(\frac{c_{p,g,f} \mu_{g,f}}{k_{g,f}} \right)^{0.333} \tag{4}$$

The heat flux through the gas film is computed by means of Newton's law of cooling:

$$q = \frac{Q}{S_w} = h_{g,f} (T_{g,w,ad} - T_{g,w}) \tag{5}$$

In this equation, the adiabatic combustion-gas wall temperature $T_{g,w,ad}$ is defined as

$$T_{g,w,ad} = T_{g,s} + \delta_{ad} \left[\frac{(u_{g,s})^2}{2 g J c_{p,g,s}} \right]$$

Since total, or stagnation, gas temperature is commonly defined as

$$T_{g,t} = T_{g,s} + \frac{(u_{g,s})^2}{2 g J c_{p,g,s}}$$

E-150

then the relation for $T_{g,w,ad}$ may be conveniently written as

$$T_{g,w,ad} = T_{g,s} + \delta_{ad}(T_{g,t} - T_{g,s}) \tag{6}$$

In a turbulent boundary layer, the value of δ_{ad} increases with Reynolds number to approximately 0.90 (ref. 3). The range of Reynolds numbers encountered in this study dictated the use of 0.90 for δ_{ad}.

It is assumed that the heat flow is circumferentially uniform at every plane perpendicular to the longitudinal centerline of the engines; that is, no distortion of heat flow is caused by the presence of supporting webs (fig. 1). In addition, since constant coolant-side engine wall temperatures are specified in the designs to be discussed, axial heat-conduction effects are assumed to be negligible.

Engine walls. - The wall separating the combustion system from the cooling system is considered in this analysis to be of 0.020-inch-thick pure nickel. In addition, the webs in each engine considered (fig. 1) are assumed to be 0.042 inch thick; but, since their effect on heat flow is assumed negligible, the web material need not be specified here. Essentially, the web dimensions affect only the coolant-passage flow area and the hydraulic diameter.

On the basis of the small thickness and high thermal conductivity of the wall, it is assumed that the steady-state heat-transfer condition is established very quickly after the beginning of combustion; and, consequently, transient effects are assumed to be negligible.

Steady-state heat transfer through the wall of a tube may be described by a form of Fourier's law (ref. 3) as

$$Q = k_w \left(\frac{2r_m l}{r_o - r_i} \right) (T_{w,i} - T_{w,o}) \tag{7}$$

If the tube of concern has a wall thickness very small in comparison to tube radius, elementary manipulations will readily show that, for the cooled engine considered here, equation (7) may be written as

$$q = \frac{Q}{S_w} = \frac{k_w}{t_w} (T_{g,w} - T_{l,w}) \tag{8}$$

Since the temperature dependence of the thermal conductivity of pure nickel is not great, the value of k_w is assumed to be sufficiently well defined by the arithmetic average of the two wall surface temperatures, as opposed to the true mean temperature. In addition, because of

the small wall thickness, and for simplicity, the inside wall surface is assumed to be the heat-transfer surface area, as opposed to the logarithmic mean suggested by equation (7).

Ceramic or carbon engine wall linings. - In some of the engines considered in this analysis, it was found necessary to augment regenerative cooling with a suitable ceramic interior wall lining. In the engines using JP-4 and oxygen as a propellant combination, a carbon film forms on the interior walls as a normal part of the combustion process during fuel-rich operation. In either event, the result is an additional heat barrier, the effect of which is quite significant because of the relatively low thermal conductivity of the linings.

By means of a development identical to that discussed for the engine wall, and using similar assumptions, the steady-state heat transfer through a coating may be shown to be described by the relation

$$q = \frac{k_c}{t_c}\left(T_{g,c} - T_{g,w}\right) \tag{9}$$

Since the thermal conductivity of the ceramic used and of carbon is essentially constant over a wide temperature range, variation of this property with temperature is assumed to be negligible.

Engine walls to coolant. - As on the combustion-gas side, the heat-transfer mechanism between engine walls and coolant is assumed to be that for fully developed turbulent flow in a tube. Again, the correlation (eq. (1)) is employed, and again the coolant transport properties are evaluated at the film temperature. Taking the film temperature to be the arithmetic average between coolant free-stream and wall temperatures, the equation for this quantity is

$$T_{l,f} = 0.5(T_{l,w} + T_l) \tag{10}$$

and equation (1) may be written for this application as

$$\frac{h_{l,f}\bar{D}_l}{k_{l,f}} = 0.023\left(\frac{G_l\bar{D}_l}{\mu_{l,f}}\right)^{0.8}\left(\frac{c_{p,l,f}\mu_{l,f}}{k_{l,f}}\right)^{0.333} \tag{11}$$

Heat flux through the coolant film is computed, as before, by means of the relation

$$q = \frac{Q}{S_w} = h_{l,f}\left(T_{l,w} - T_l\right) \tag{12}$$

From energy balance considerations, the equation that relates the coolant temperature to axial location in the coolant jacket is

$$T_l = \left(\frac{q + q_0}{2}\right) \frac{S_q}{w_l \bar{c}_{p,l}} + T_{l,0} \tag{13}$$

where $\bar{c}_{p,l}$ is evaluated at $0.5(T_l + T_{l,0})$ for a specific pressure. Then, the temperature of the coolant at a given location is a function of the coolant temperature at some previous location, the average heat flux between the two locations concerned, the corresponding heat-transfer area, the coolant-flow rate, and the mean specific heat.

Pressure-Drop Calculations

For the purpose of determining the pressure loss of the coolant as it passes through its jacket, the individual coolant channels (see fig. 1) are assumed to be straight tubes. The relation used to compute the pressure loss between any two axial locations in the coolant jacket is the familiar form

$$p_l - p_{l,0} = \frac{2G_{l,m}^2 f l}{g \bar{D}_{l,m} \rho_{l,m}}$$

where

$$G_{l,m} = 0.5(G_l + G_{l,0})$$

$$\bar{D}_{l,m} = 0.5(\bar{D}_l + \bar{D}_{l,0})$$

f is determined for a specific $\bar{D}_{l,m}$, $\rho_{l,m}$ is evaluated at

$$T = 0.5(T_l + T_{l,0})$$

and

$$p = 0.5(p_l + p_{l,0})$$

Generally, the Fanning friction factor f is considered to be a function of flow Reynolds number and of hydraulic diameter. In its application to the coolant flow in this study, however, since for a given hydraulic diameter the value of the friction factor varies but little in the Reynolds number range encountered (approximately 1.5×10^6), it is assumed to be a function of hydraulic diameter only for a specific tube surface condition. A plot of this function appears in figure 2.

PROCEDURES

Parameters Studied

Engine size, combustion-chamber pressure, contraction and expansion area ratios. - As an index of engine size, the thrust-level range covers from 1000 to 1,000,000 pounds. The combustion-chamber pressure varies from 60 to 600 pounds per square inch absolute, and contraction and expansion area ratios are varied from 1.5 to 3 and from 3.8 to 50, respectively.

Propellant combinations. - Four of the propellant combinations, H_2-F_2, H_2-O_2, N_2H_4-F_2, and NH_3-F_2, were selected because they are high-energy combinations of general current interest. The other, JP4-O_2, not generally considered a high-energy combination, was chosen as representative of those in more common use for comparison purposes.

Fuel-oxidant mixture ratio. - The range of fuel-oxidant mixture ratio considered for three of the propellant combinations under investigation (H_2-F_2, N_2H_4-F_2, and JP4-O_2) is from the stoichiometric point to or slightly past the more fuel-rich mixture ratio corresponding to the condition of maximum characteristic velocity. It was assumed that the H_2-F_2 data would adequately define trends that would, in general, also describe the H_2-O_2 system, and similarly, that the N_2H_4-F_2 data would sufficiently describe the NH_3-F_2 system.

Performance efficiency. - Certain inefficiencies within the rocket engine, such as nonhomogeneity of the propellant mixture, incomplete combustion, and others, prevent the full ideal performance of the propellant combination from being realized. Therefore, the ideal performance of the engine must be modified by means of a performance efficiency factor that must be experimentally determined. In this study, the performance efficiency η is defined as

$$\eta = \frac{c^*_{ac}}{c^*_{id}}$$

Since the characteristic velocity is directly proportional to specific impulse, which in turn is directly proportional to the square root of the combustion temperature (ref. 5), a decrease in performance is manifested by a corresponding decrease in combustion temperature if the molecular weight of the products of combustion and the pressure remain constant. This relation is described by the equation

$$T_1 = \eta^2 T_{1,id}$$

Further, for an engine of fixed geometry to maintain the design combustion-chamber pressure at a performance efficiency less than 1.00, the propellant flow rate must be increased proportionately. This adjustment of flow rate may be computed by the relation

$$w_p = \frac{p_1 A_2 g}{\eta c^*_{id}}$$

The performance efficiency range considered in this study is from 90 to 100 percent, a range considered representative of practical rocket-engine application.

E-150

Temperature Ranges and Limitations

The pertinent physical properties of the materials involved in this analysis are discussed in detail in appendix B. Some important temperature limitations covered in that section, along with some basic assumptions not discussed heretofore, are presented at this point for convenience.

CJ-2

The maximum safe allowable bulk temperature limits for hydrazine, ammonia, and JP-4 are designated as 950°, 600°, and 950° R, respectively. The maximum bulk temperature for hydrogen for a coolant is here considered to be 1100° R. This value was arrived at by considering a reasonable temperature drop through the engine-wall material and the coolant film from the design temperature of the engine wall on the combustion-gas side, which was 1460° R. This design wall temperature was selected as a conservative value for the material concerned, which is, as stated earlier, pure nickel. For simplicity, 1100° R is also assumed to be the temperature limit for fluorine and oxygen, although practical limitations (such as the possibility of rapid oxidation of the engine-wall material) may actually fix this limit at some lower level.

The temperature at which the coolant is supplied to the engine coolant jacket varies with the coolant itself. Hydrazine and JP-4 are here assumed to be supplied at 530° R, essentially sea-level atmospheric temperature, while ammonia is assumed to be available at 435° R, the temperature it would attain (approximately) if allowed to boil at atmospheric pressure. Hydrogen would be supplied at 60° R, a temperature near its critical point, and oxygen would be available at 163° R, which is approximately its boiling point at atmospheric pressure. Fluorine, requiring auxiliary cooling, is assumed to be supplied at 140° R, approximately the boiling point of nitrogen at atmospheric pressure. It is presumed that the fluorine container would be surrounded by a liquid-nitrogen jacket.

Maximum Specific Cooling Potential

In order to facilitate the study of the effects on regenerative-cooling requirements of changes in several of the rocket-engine design parameters, it will be convenient at this point to define a quantity that will be useful in this regard. By means of this index, it will be possible to gain some quantitative concept of the relative ability of the propellants of concern here to cool the engines considered. This index is the maximum specific cooling potential ψ_{max} of the propellant component.

The maximum specific cooling potential of a coolant is directly related to the heat it acquires as it rises from its supply temperature to its upper temperature limit. This value, as used in this study, is defined as the total heat absorbed by the coolant per second divided by the cross-sectional area of the engine nozzle throat. This quantity has the units Btu/(sec)(sq in.) and may be written

$$\psi_{max} = \frac{w_l}{A_2} \int_{T_{in}}^{T_{max}} c_p \, dT = \frac{F\theta}{IA_2\eta} (H_{max} - H_{in})$$

This computation assumes that c_p for the coolant is substantially independent of pressure over the relatively small pressure range the coolant encounters in the engine cooling jacket, and is dependent only on temperature. The maximum specific cooling potential is a useful index because it can be used to compare the specific-heat capacity of various coolants and is independent of the engine geometry and size.

The values of ψ_{max} for the propellants considered in this study are compared in figure 3. The combustion-chamber pressure for each case is 300 pounds per square inch absolute, and the engines are geometrically identical, having a nominal thrust level of 100,000 pounds. The fuel-oxidant mixtures considered are those for maximum theoretical characteristic velocity, which is a convenient arbitrary reference point. These mixtures, in percent fuel by weight, are 15.03, 23.95, 31.91, 24.93, and 30.59 for H_2-F_2, H_2-O_2, N_2H_4-F_2, NH_3-F_2, and JP4-O_2, respectively. Figure 3 shows clearly the superiority of hydrogen as a regenerative coolant in either of the two combinations shown. This is due to the fact that hydrogen's specific heat is much higher that that of the other coolants, as will be examined later. In addition, hydrogen's allowable temperature rise is much greater than that of the noncryogenic coolants considered. The darkened areas on the bars for fluorine and oxygen in figure 3 indicate the maximum cooling potentials of those two oxidants if boiling of the coolant is to be avoided. In that case, the upper allowable bulk temperature limits for fluorine and oxygen are 235° and 250° R, respectively. These temperatures represent the approximate boiling points of

the two oxidants at 400 pounds per square inch absolute, the nominal pressure in the coolant jackets of the engines considered in figure 3.

Because, in general, the cooling characteristics of the oxidants are much inferior to those of the fuel components, the engines considered in this study are all assumed to be fuel-cooled.

E-150

Cooling Utilization Ratio

For the purpose of evaluating the cooling requirements of the engines considered here, it is convenient to define another quantity, a cooling utilization ratio. This quantity is the ratio of the amount of heat rejected from a cooled engine ψ_{ac} to the amount of heat the coolant is capable of absorbing. For successful cooling, then, the cooling utilization ratio must not exceed the value 1.0. In general, a low ratio would indicate that an engine may be cooled regeneratively with relative ease, while a ratio near 1.0 would indicate that the cooling is marginal. The ratio as used in this report is defined as

CJ-2 back

$$\varphi = \frac{\psi_{ac}}{\psi_{max}} = \frac{H_{out} - H_{in}}{H_{max} - H_{in}}$$

Engine Design

Engine type considered. - The type of regeneratively cooled engine considered in this analysis is shown schematically in figure 1. It is recognized as a simple cylindrical engine having a single-pass, axial-flow cooling jacket. A variety of other engine shapes and cooling jacket configurations exists, of course, some of which may have advantages over this type of design. The one chosen, however, is thought to be adequate for the present study and will doubtless display cooling demands and characteristics that will generally be common with most other engines and cooling schemes.

Referring again to figure 1, the coolant enters the cooling jacket from a manifold located at the nozzle exit. It then moves axially along the engine until it encounters another manifold at the injector location, from which point it is introduced into the combustion chamber and subsequently burned. During its passage along the engine wall, even distribution of the coolant circumferentially is accomplished by means of a relatively large number of evenly spaced radial webs that separate the engine wall from the coolant jacket outer wall and form many flow channels. Of course, the heat transferred to the coolant is not wasted, since it adds to the heat content and subsequently to the energy level of the propellant before combustion.

Rocket-engine design (exclusive of cooling system). - The specific designs of the engines considered in this analysis were determined through consideration of basic continuity and momentum concepts. Combining the defining relations (ref. 5) for characteristic velocity,

$$c^* = \frac{p_1 A_2 g}{w_p} = \frac{Ig}{C_F}$$

and for specific impulse,

$$I = \frac{F}{w_p}$$

the nozzle throat area may be expressed as

$$A_2 = \frac{c^* F}{p_1 g I} \tag{14}$$

The values of c^* and I are characteristic of propellant combination, fuel and oxidant mixture ratio, and combustion pressure, and are assumed for the purposes of this study to be those for shifting equilibrium composition of the combustion products through the engine.

When the nozzle throat area is defined, the combustion-chamber diameter may be readily computed by means of the desired contraction ratio. Chamber length, for this study, was determined by a simple consideration of the length thought necessary for fuel and oxidant mixing and combustion, and the shape of the convergent section of the nozzle was chosen as a smooth, well-rounded curve. The nozzle expansion ratio, or ratio of the cross-sectional area of the nozzle exit to that of the throat, is fixed by design altitude requirements, and the nozzle length is then a function of nozzle shape. The nozzle type assumed for this study is conical, and the divergence half-angle is 15°, a value considered to be optimum with respect to wall friction losses, radial velocity components, and separation and turbulence losses (ref. 5).

Cooling-system design considerations. - Heat transfer from the engine to the coolant depends to a large extent on the heat-transfer coefficient between the cooled surface and the coolant itself. The heat-transfer coefficient, in turn, is greatly dependent on the velocity with which the coolant passes along the heat-transfer surface. Then, an important criterion is the coolant-passage height, for this dimension largely determines the flow cross-sectional area and consequently the flow velocity of the coolant. The coolant-passage height must be compromised between the good heat-transfer qualities associated with high coolant velocity (low passage height) and the converse requirement of low pressure-loss characteristics associated with low coolant-flow velocity (large passage height).

Calculation Procedure

It was necessary to design a relatively large number of engines to investigate the cooling-requirement effects of the large spectrum of design parameters indicated for study. It was decided arbitrarily to base the design schedule on nozzle throat area, in part because of the close relation between this dimension and engine size, which will be shown to be of major importance in determining cooling requirements. Four basic nozzle throat areas were specified, corresponding nominally to sea-level thrust values of 1000, 10,000, 100,000, and 1,000,000 pounds. In addition, three other throat areas were specified for engines operating at different combustion-chamber pressures while maintaining the nominal (100,000-lb) thrust level of the engine operating at the reference pressure of 300 pounds per square inch absolute. If the engines had been designed to produce a specified uniform series of thrust values, a separate configuration would have been required for each examined condition, resulting in many more designs than were actually made. Such a task was beyond the intended scope of this study. Figure 4 presents in tabular form the pertinent dimensions of the engines designed for this study.

Each of the engines was arbitrarily divided into a relatively large number of sections along the longitudinal centerline; the number of sections was a function of over-all engine length, the actual number varying from 15 to 26. In general, the sections were closely spaced at regions of high heat flux and/or geometry change rates, such as at the nozzle throat, and spaced farther apart in regions of more uniform conditions, such as near the injector end of the combustion chamber or near the nozzle exit.

At each of the selected stations, a complete heat-transfer analysis was performed, based upon the calculation techniques described elsewhere in this report. In general, the calculations were based on a required engine-wall temperature, specified either on the combustion-gas side or the coolant side of the engine wall. If the coolant were a cryogenic fluid, such as liquid hydrogen, then the temperature limit indicated would be the metallurgical temperature limit on the combustion-gas side of the nickel engine wall specified here as 1460° R. However, if the coolant were hydrazine, ammonia, or JP-4, the boiling or degradation temperature limits of these coolants, identified elsewhere in this report, would determine the coolant-side engine-wall temperature. In either case, the design criterion was clearly established, and the calculation procedure then ultimately led to the determination of a coolant-jacket design that would cause the desired engine-wall temperature to occur. If it were indicated that the desired degree of cooling was not possible by these means, it would become necessary to assume a ceramic wall liner, as discussed earlier, to achieve a successful design. Of course, the impossibility of a solution indicated an area where simple regnerative fuel-cooling is not feasible. Attaining knowledge of these areas was one of the intended purposes of this study.

In addition to the heat-transfer analysis, the pressure loss of the coolant was computed. As pointed out earlier, in an effort to keep the analysis on a practical level, a major requirement of a successful engine design was that the pressure loss of the coolant must be within reasonable limits. If a design exhibited a coolant-jacket pressure loss of more than about 100 pounds per square inch, the design was arbitrarily considered impractical, regardless of the computed heat-transfer characteristics. The coolant pressure drops for the engine designs considered are presented in tables I to VI.

The calculations were done on a high-speed electronic digital computer.

RESULTS AND DISCUSSION

Figure 5 presents a typical summary of a complete evaluation of a proposed engine. The engine pictured here is identified as engine A in figure 4. Its propellant combination is H_2-F_2, 15.03 percent hydrogen by weight, and its nominal thrust level is 100,000 pounds. The engine combustion-chamber pressure is 300 pounds per square inch absolute, and the design uniform combustion-gas-side wall temperature is 1460° R with entering coolant (H_2) at 60° R and 378 pounds per square inch absolute. The profiles shown, representing only a small fraction of the number of quantities calculated, are heat flux, coolant temperature and velocity, and coolant-jacket height.

The remaining portions of this report will discuss the effects of the engine design parameters of concern on cooling requirements, with emphasis on trends rather than the absolute values computed, since the values are obviously quite sensitive to the design criteria selected. The general trends, on the other hand, are felt to be indicative of actual tendencies and sensitive only to the basic underlying assumptions of the calculation technique.

Effect of Propellant Combination and Engine Size

The relation between cooling utilization ratio and engine size is shown for several propellant combinations in figure 6. In all cases, the cooling utilization ratio φ decreases as engine thrust, indicated by nozzle throat cross-sectional area, increases. The reason for this tendency is straightforward. At constant combustion pressure, the coolant (fuel) flow rate is increased by an amount proportional to the square of the increase of the throat diameter, while the engine heat-transfer surface area is increased by an amount proportional to the first power of the increase of the throat diameter. In addition, an examination of

equation (4) indicates that a larger diameter engine has a lower combustion-gas-side heat-transfer coefficient, and consequently a lower heat flux, than a smaller one. These two effects combine to produce the curve trends shown.

The propellant combinations H_2-F_2, H_2-O_2, and JP4-O_2 display the ability, according to the methods of this study, to be regeneratively cooled throughout the entire size range shown in figure 6, encompassirg a thrust range from about 1000 to 1,000,000 pounds. Again, it should be noted that the JP4-O_2 engine is considered to have a 0.01-inch-thick carbon lining on the interior walls. If combustion conditions or other influencing factors should prevent the formation of this assumed carbon layer, then the cooling of this engine would certainly become more difficult to accomplish, and possibly would not even be feasible for some small engines.

Figure 6 indicates that, of the NH_3-F_2 engines considered, only the larger ones may be regeneratively cooled with confidence by the methods assumed here, even with the addition of a ceramic engine liner. If, however, vaporization of the ammonia were utilized in the cooling process, the cooling capacity of this coolant would be increased by a factor of about 3, allowing much smaller engines to be cooled. A somewhat less pessimistic picture is presented for the N_2H_4-F_2 engine, where only small engines have cooling utilization ratios greater than 1.0. In conjunction with figure 6 and subsequent curves, a brief summary of some of the more important of the calculated quantities pertaining to the curves is presented in tables I to VI.

Effect of Performance Efficiency

The results of this study indicate that performance efficiency influences regenerative-cooling requirements greatly. Figure 7 illustrates the trends indicated by the calculations. In examining this figure it is seen that a reduction of 10 percent (from 100 to 90 percent) in performance efficiency results in a reduction in cooling utilization ratio of approximately 30 percent for each of the three propellant combinations shown. For a given engine configuration and thrust level, a decrease in performance efficiency is accompanied by an increase in fuel (coolant) flow rate and a decrease in combustion temperature. As a consequence, the coolant experiences a smaller temperature rise and the cooling utilization ratio is therefore lower.

Effect of Fuel-Oxidant Mixture Ratio

According to the results of this analysis, the relative amount of fuel in the propellant mixture is another extremely influential engine design parameter with respect to cooling requirements. In figure 8, the slopes of the curves indicate the extreme sensitivity of this relation.

In the case of H_2-F_2, for example, a decrease in fuel content from 15 to 5 percent (approximately stoichiometric) results in an increase in cooling utilization ratio of over 400 percent. The reason for this tendency is immediately apparent. The highest combustion temperature occurs near the stoichiometric point; and, of course, a relatively low coolant (fuel) flow occurs at this point. As the proportion of fuel in the propellant mixture increases, the combustion temperature decreases and more coolant becomes available. The net result is a gradual reduction of temperature rise of the coolant as the fuel-oxidant mixture becomes more and more fuel-rich than near the stoichiometric point. The nature of this relation suggests that situations might arise where a compromise between the desirability of operating at or very near the stoichiometric point and operating at a somewhat higher fuel-oxidant mixture ratio for the sake of cooling would be advantageous. One such compromise might be to use an injector that would cause the propellant mixture immediately adjacent to the engine walls to be fuel-rich, while the main bulk of the propellant mixture is more nearly stoichiometric.

Effect of Expansion Area Ratio

An increase in nozzle expansion ratio in an otherwise fixed engine configuration results in an increase in cooling requirements in the range investigated in this study, as shown in figure 9. The cooling requirement for the N_2H_4-F_2 engine becomes large enough that the cooling utilization ratio becomes larger than 1.0, indicating difficulty in regeneratively cooling this engine, according to the calculation method of this study. The limiting expansion ratio of about 16 for the N_2H_4-F_2 engine shown in figure 9 is for the noted size engine only; a larger engine would have a higher limiting expansion ratio for successful regenerative cooling, and a smaller engine would have a lower limiting ratio.

The trend of the curves of figure 9 is due to the increase in heat-transfer surface area necessarily resulting from an increase in nozzle expansion ratio, maintaining the stated divergence half-angle of 15°. While it is true that the heat-transfer rate to the nozzle walls decreases at successive points through an expanding nozzle because of the decreasing combustion-gas bulk, or stream temperature, the net effect produces the curve trends shown.

Effect of Combustion-Chamber Pressure

The relation between cooling utilization ratio and combustion-chamber pressure for three propellant combinations is illustrated in figure 10. For fixed engine geometry, a decrease in cooling utilization ratio results from an increase in chamber pressure. This tendency is

due to the necessary proportional increase in propellant flow rate, and consequently coolant flow rate, with chamber pressure, while the combustion temperature and combustion-gas-side heat-transfer coefficient increase at a much lower rate. As a result, more coolant becomes available with a higher chamber pressure, while heat flux has increased by a lesser amount proportionately. The net effect is that the coolant experiences a smaller temperature rise than at a lower chamber pressure, and the cooling utilization ratio therefore decreases.

For a constant thrust condition, the relation between cooling utilization ratio and combustion-chamber pressure was somewhat modified because, to maintain a constant thrust level, engine size was necessarily reduced as combustion-chamber pressure was increased, as is indicated by equation (14). Referring to the earlier discussion of the influence on cooling requirements of engine size, it will be recalled that, in general, large engines may be regeneratively cooled more readily than smaller ones. This tendency, then, explains the relative positions of the curves of figure 10. Below the reference combustion pressure of 300 pounds per square inch absolute, the dashed curves (representing constant thrust) fall below the solid curves (representing constant engine size), because larger engines were needed. Above 300 pounds per square inch absolute, where smaller engines were required, a greater cooling load is indicated, and the constant thrust curves lie above the constant engine size curves. It will be noted that the curves for JP4-O_2 are oriented somewhat differently from those of the other two combinations. This difference is due to the large (increasing) temperature variation of the carbon engine lining with pressure increase, while engines using the other two combinations exhibit a more nearly constant wall surface temperature with pressure variation.

The curves for N_2H_4-F_2 and JP4-O_2 in figure 10 are not shown for the maximum characteristic velocity condition as in the other figures, since sufficient thermodynamic data at that fuel-oxidant mixture ratio were not available. The fuel-oxidant mixture ratios presented in this figure, however, closely approximate the maximum characteristic velocity condition.

Effect of Contraction Area Ratio

Figure 11 presents the results of the study of the effect of engine contraction ratio on cooling utilization ratio. Varying the contraction ratio from 1.5 to 3 in an otherwise fixed engine configuration for the three propellant combinations shown produces only very small changes (4 percent maximum) in cooling load. On the basis of these observations, it must be concluded that the contraction ratio variation, in the cases studied here, has no significant effect on cooling utilization ratio.

E-150
CJ-3

SUMMARY OF RESULTS

An analysis was made of the regenerative-cooling requirements of rocket engines. Each of seven parameters was varied independently to evaluate its significance in cooling considerations. Results were as follows:

1. The propellant combinations of H_2-F_2, H_2-O_2, N_2H_4-F_2, NH_3-F_2, and JP4-O_2 were studied. Considering the fuels as coolants, H_2 offered the greatest reserve cooling capacity relative to the cooling needs; NH_3 offered the least cooling capacity.

2. Increasing nozzle throat cross-sectional area, and consequently engine thrust level, increased cooling capability.

3. For a specific engine design and propellant combination, the most influential parameter on regenerative-cooling requirements was performance efficiency. In general, a small decrease in efficiency resulted in a relatively large decrease in cooling requirements.

4. As the proportion of fuel in the propellant combinations was increased beyond the stoichiometric ratio, the relation between cooling capacity and engine cooling requirements became more favorable.

5. The next most significant parameter was the nozzle expansion area ratio; increasing this ratio made cooling more difficult, particularly with fuels of less reserve cooling capacity.

6. Increasing combustion pressure, and consequently thrust, with fixed engine geometry tended to improve cooling capability; increasing combustion pressure and engine size at constant thrust either reversed or lessened this tendency.

7. Varying engine contraction area ratio from 1.5 to 3 had no significant effect on regenerative-cooling requirements.

Lewis Research Center
National Aeronautics and Space Administration
Cleveland, Ohio, June 25, 1959

E-150

APPENDIX A

SYMBOLS

A	cross-sectional area, sq in.
C_F	thrust coefficient, F/A_2p_1, dimensionless
c^*	characteristic exhaust velocity, in./sec
c_p	specific heat at constant pressure, Btu/(lb)($^\circ$R)
$\bar{D}$	hydraulic diameter, 4A/wetted perimeter, in.
F	thrust, lb
f	Fanning friction factor, dimensionless
G	flow flux, w/A, (lb/sec)/sq in.
g	gravitational conversion factor, 386.4 (lb mass/lb force)(in./sec^2)
H	coolant enthalpy, Btu/lb
h	heat-transfer coefficient, Btu/(sq in.)(sec)($^\circ$R)
I	specific impulse, F/w, lb-sec/lb
J	mechanical equivalent of heat, 9336 in.-lb/Btu
k	thermal conductivity, Btu/(in.)(sec)($^\circ$R)
l	flow length, in.
Nu	Nusselt number, $h\bar{D}/k$, dimensionless
Pr	Prandtl number, $c_p\mu/k$, dimensionless
p	pressure, lb/sq in.
Q	heat flow, Btu/sec
q	heat flux, Btu/(sec)(sq in.)
R	gas constant, in./$^\circ$R
Re	Reynolds number, $\rho u\bar{D}/\mu$, dimensionless

E-150
CJ-3 back

r	radius, in.
S	surface area, sq in.
T	temperature, ^{o}R
t	thickness
u	velocity, in./sec
w	weight-flow rate, lb/sec
Z	compressibility factor, $p/\rho RT$, dimensionless
δ_{ad}	adiabatic recovery factor, dimensionless
η	performance efficiency, dimensionless
θ	weight fraction of fuel in propellant mixture
μ	dynamic viscosity, lb/(sec)(in.)
ρ	density, lb/cu in.
φ	cooling utilization ratio, dimensionless
ψ	specific cooling potential, Btu/(sec)(sq in.)

Subscripts:

ac	actual
ad	adiabatic
c	ceramic
f	film
g	gas
i	inside
id	ideal
in	coolant-supply (cooling jacket inlet) station
l	coolant

m	mean
max	maximum
o	outside
out	coolant at injector (cooling jacket outlet) station
p	propellant
q	heat transfer
s	stream or bulk
t	total
w	wall
0	previous location
1	combustion chamber
2	nozzle throat
3	nozzle exit

APPENDIX B

PHYSICAL PROPERTIES OF MATERIALS INVOLVED IN STUDY

The worth of a study of this nature is related not only to the soundness of the assumptions made and the calculations used, but also to the degree of accuracy with which the properties of the materials involved are known. As a consequence, the sources of the property values used in this report are cited here in detail. In addition, some assumptions that were necessarily made during the study will be outlined here.

Where no curves of the physical properties used appear in conjunction with the following sections, the data may be obtained directly from the references cited or from the text of this report. Curves are presented where they represent a compilation of information from more than one source, where sections of them have been interpolated or extrapolated on the basis of comparison with known characteristics of other similar materials, or where units have been changed from those of the source for consistency with other phases of the study.

Combustion Gases

At the present time, very little or no experimental data exist for the properties of the products of combustion of the propellant combinations of interest here. However, a general method has been established (ref. 6) that permits the calculation of the required properties on the assumption that chemical equilibrium exists among the products of combustion.

The transport properties of the propellant combination products (i.e., specific heat, viscosity, and thermal conductivity) were obtained from references 7 to 12. In their application to this analysis, it was assumed that these properties vary with temperature only. It is thought that the error introduced by the use of this assumption is small, since the properties concerned are generally considered to have a strong pressure dependence only near their critical points.

Ceramic and Carbon Engine-Wall Linings

Where it was necessary to specify an internal engine lining of ceramic, a stabilized (cubic form) zirconia ceramic was selected because of its high chemical resistance, very low thermal conductivity, and high melting point (ref. 13). Although the manufacturer's specifications suggest coating thicknesses of from 0.005 to 0.05 inch, a conservative

E-150

thickness of 0.01 inch was selected for this study. The specified thermal conductivity over a wide temperature range is 1.543×10^{-5} Btu/(sec)(in.)($^{\circ}$R), and this value is here considered to be constant for any temperature. The manufacturer also gives the melting point of this material as approximately 4960° R, which of course establishes the absolute upper local design temperature for this material.

During the usual fuel-rich combustion of JP-4 and oxygen in a rocket engine, a thin carbon film has been observed to form over the surfaces contacted by the combustion gases. Experimental investigations at the Lewis Research Center have led to the conclusion that this film thickness is effectively of the order of 0.01 inch, and this value has been assumed in this study. Thermal conductivities reported for carbon vary from 9.25×10^{-7} (lampblack) to 6.95×10^{-5} (petroleum coke) Btu/(sec)(in.)($^{\circ}$R). The value assumed for this analysis was 7.0×10^{-6} Btu/(sec)(in.)($^{\circ}$R), a value suggested by the results of some limited investigations at this laboratory.

Engine Walls

Pure nickel was selected for the wall material of every engine considered in this report. Other than in consideration of its relatively high thermal conductivity, it was chosen because of its excellent resistance to corrosive atmospheres and its reasonably good strength characteristics at high temperatures. In addition, it brazes well, is ductile, and has favorable work-hardening characteristics (ref. 14), thereby lending itself well to engine construction. The average thermal conductivity of this material over the temperature range encountered is approximately 8×10^{-4} Btu/(sec)(in.)($^{\circ}$R), a value significantly higher than those for other materials that might be considered for their strength, such as stainless steel. The calculation procedure utilized in this study considered the variation of thermal conductivity with temperature, the required data being taken from reference 3.

Coolants

In addition to the transport properties required for heat-transfer calculations, the additional requirement of pressure-loss calculations for the coolant necessitates that the density characteristics be known also.

In all cases except for ammonia, the engine coolant-side wall temperature was allowed to attain a temperature about 50° R higher than the stated maximum allowable coolant bulk temperature. This fairly common practice is based on the premise that only the layer of coolant immediately adjacent to the wall is subjected to this temperature at any

time, and the rapid mixing that is characteristic of a turbulent boundary layer prevents any specific part of the coolant from remaining at this temperature level for any significant period of time.

Hydrogen. - An estimate of the hydrogen storage time for a practical rocket-engine application would indicate that the hydrogen would be approximately 95 percent (or higher) in the para form (ref. 15) at the initiation of operation. Since the stay time of the hydrogen in the engine cooling jacket is extremely short (average velocities in the order of 250 ft/sec), time would prevent an equilibrium mixture of the ortho and para modifications from being established. In view of this, the properties shown in figure 12 are those for hydrogen in approximately 95 percent para, 5 percent ortho form. The properties in this figure were taken from references 15 and 16.

Hydrazine. - Reference 17 is the principal source of the physical property data of very pure (97 to 100 percent) anhydrous hydrazine used here, with one exception. The single value for thermal conductivity shown in the physical property curves (fig. 13) was determined from some limited experimental investigations. Depending upon materials in contact, pressure, purity, rate of heating, and perhaps other as yet unidentified factors, hydrazine begins, in the absence of an oxidant, to decompose into nitrogen, ammonia, and in some cases hydrogen at a temperature of the order of 950° R. At the pressure anticipated in the coolant jackets of the engines considered, the decomposition temperature is very nearly the boiling temperature of hydrazine (approx. 900°, 950°, and 1020° R at 225, 375, and 750 lb/sq in. abs, respectively). Consequently, the maximum design value for the coolant-jacket wall temperature was established at 1000° R.

Ammonia. - The physical properties of pure liquid ammonia used in this study were taken from reference 18 and are shown in figure 14. Since ammonia was considered only for engines having a combustion-chamber pressure of 300 pounds per square inch absolute, the maximum bulk temperature ammonia could be allowed to reach as a coolant was 600° R. This temperature corresponds to the boiling point of ammonia at a coolant-jacket pressure of approximately 375 pounds per square inch absolute. To limit the ammonia bulk temperature to 600° R, the engines were designed to have a maximum coolant-jacket wall temperature of 700° R, since the calculations indicated an average temperature drop through the coolant heat-transfer interface of approximately 100° R.

JP-4 Fuel. - Experience with turbojet engines has indicated generally that the maximum bulk temperature that the JP-4 coolant can be safely allowed to attain is approximately 900° R. Above that temperature, in the absence of an oxidant, JP-4 begins to "coke," or precipitate gums and varnishes that tend to build up and eventually block fuel-nozzle

holes and perhaps the coolant-jacket passages. However, the coking process depends on time at temperature as well as temperature itself; and, since the coolant residence time in a rocket-engine cooling jacket is much shorter than in a turbojet oil cooler, the coking temperature for this study was assumed to be 950° R. Since JP-4 begins to boil at approximately 1090° at a cooling-jacket pressure of 375 pounds per square inch absolute, the coking threshhold temperature is necessarily the maximum coolant bulk temperature allowable in a successful engine design. Accordingly, the maximum coolant-side wall design temperature was established at 1000° R.

The physical property data for JP-4 used here were taken from references 19 and 20 and are shown in figure 15.

Fluorine. - Since the oxidants were only briefly examined with respect to cooling, a complete schedule of their properties was not required. References 21 to 23 supplied the necessary specific-heat data for the limited study. These data are presented in figure 16.

Oxygen. - References 24 and 25 are the sources of the specific-heat data for oxygen, which appear in figure 17.

REFERENCES

1. Bartz, D. R.: A Simple Equation for Rapid Estimation of Rocket Nozzle Convective Heat Transfer Coefficients. Jet Prop., vol. 27, no. 1, Jan. 1957, pp. 49-51.

2. McAdams, William H.: Heat Transmission. Second ed., McGraw-Hill Book Co., Inc., 1942.

3. Eckert, E. R. G.: Introduction to the Transfer of Heat and Mass. McGraw-Hill Book Co., Inc., 1950.

4. Schlichting, Hermann: Boundary Layer Theory. McGraw-Hill Book Co., Inc., 1955.

5. Sutton, George P.: Rocket Propulsion Elements. Second ed., John Wiley & Sons, Inc., 1956.

6. Huff, Vearl N., Gordon, Sanford, and Morrell, Virginia E.: General Method and Thermodynamic Tables for Computation of Equilibrium Composition and Temperature of Chemical Reactions. NACA Rep. 1037, 1951. (Supersedes NACA TN's 2113 and 2161.)

7. Fortini, Anthony, and Huff, Vearl N.: Theoretical Performance of Liquid Hydrogen and Liquid Fluorine as a Rocket Propellant for a Chamber Pressure of 600 Pounds per Square Inch Absolute. NACA RM E56L10a, 1957.

E-150

CJ-4

8. Gordon, Sanford, and Huff, Vearl N.: Theoretical Peformance of Liquid Hydrogen and Liquid Fluorine as a Rocket Propellant. NACA RM E52L11, 1953.

9. Gordon, Sanford, and McBride, Bonnie J.: Theoretical Performance of Liquid Hydrogen with Liquid Oxygen as a Rocket Propellant. NASA MEMO 5-21-59E, 1959.

10. Gordon, Sanford, and Huff, Vearl N.: Theoretical Performance of Liquid Hydrazine and Liquid Fluorine as a Rocket Propellant. NACA RM E53E12, 1953.

11. Gordon, Sanford, and Huff, Vearl N.: Theoretical Performance of Liquid Ammonia and Liquid Fluorine as a Rocket Propellant. NACA RM E53A26, 1953.

12. Huff, Vearl N., Fortini, Anthony, and Gordon, Sanford: Theoretical Performance of JP-4 Fuel and Liquid Oxygen as a Rocket Propellant. II - Equilibrium Composition. NACA RM E56D23, 1956.

13. Members of the Staff: Bull. CP11.3, Refractories Div., Norton Co., Worcester (Mass.), Nov. 28, 1955.

14. Anon.: Engineering Properties of Nickel. Tech. Bull. T-15, The International Nickel Co., Inc., July 1949.

15. Woolley, Harold W., Scott, Russell B., and Brickwedde, F. G.: Compilation of Thermal Properties of Hydrogen in Its Various Isotopic and Ortho-Para Modifications. Jour. Res. Nat. Bur. Standards, vol. 41, no. 5, Nov. 1948, pp. 379-475.

16. Friedman, Abraham S., and Hilsenrath, Joseph: The Thermodynamic and Transport Properties of Liquid Hydrogen and Its Isotopes, Pt. I. Rep. 3163, NBS, Mar. 15, 1954.

17. Clark, Charles C.: Hydrazine. Mathieson Chem. Corp., Baltimore (Md.), 1953.

18. Anon.: Tables of Thermodynamic Properties of Ammonia. Cir. 142, NBS, 1945.

19. Barnett, Henry C., and Hibbard, Robert R.: Properties of Aircraft Fuels. NACA TN 3276, 1956.

20. Smith, J. F. Downie: The Thermal Conductivity of Liquids. Trans. ASME, vol. 58, no. 8, Nov. 1936, pp. 719-725.

21. Hu, Jih-Heng, White, David, and Johnston, Herrick L.: Condensed Gas Calorimetry. V. Heat Capacities, Latent Heats and Entropies of Fluorine from 13 to 85° K; Heats of Transition, Fusion, Vaporization, and Vapor Pressures of the Liquid. Jour. Am. Chem. Soc., vol. 75, no. 22, Nov. 20, 1953, pp. 5642-5645.

22. Kanda, E.: Studies on Fluorine at Low Temperatures. VIII. Determination of Molecular Heat, Heat of Fusion of Condensed Fluorine and the Entropy of Fluorine. Bull. Chem. Soc. (Japan), vol. 12, no. 12, 1937, pp. 511-520.

23. Cole, L. G., Farber, M., and Elverum, G. W., Jr.: Thermodynamic Properties of the Fluorine Atom and Molecule and of Hydrogen Fluorine to 5000° K. Jour. Chem. Phys., vol. 20, Apr. 1952, pp. 586-590.

24. Giauque, W. F., and Johnston, H. L.: The Heat Capacity of Oxygen from 12° K to Its Boiling Point and Its Heat of Vaporization. The Entropy from Spectroscopic Data. Jour. Am. Chem. Soc., vol. 51, July 1929, pp. 2300-2321.

25. Woolley, H. W.: Thermodynamic Properties of Molecular Oxygen. Rep. 2611, NBS, June 30, 1953.

E-150

CJ-4 back

TABLE I. - SEVERAL PERTINENT CALCULATED QUANTITIES FOR ENGINES OF FIGURE 6

Variable	Over-all engine values								Conditions at throat					Cooling potential		
Throat area, A_2, sq in.	Propellant combination	Engine geometry (fig. 4)	Propellant flow rate, w_p, lb/sec	Coolant flow rate, w_l, lb/sec	Cooled surface area, S, sq in.	Average heat flux, q_m, Btu/(sec)(sq in.)	Coolant temperature rise, $T_{out} - T_{in}$, ^oR	Coolant pressure drop, $P_{in} - P_{out}$, lb/sq in.	Heat flux, q, Btu/(sec)(sq in.)	Gas-side heat-transfer coefficient, h_g, Btu/(sq in.)(sec)(^oR)	Coolant-side heat-transfer coefficient, h_l, Btu/(sq in.)(sec)(^oR)	Wall thermal conductivity, k_m, Btu/(in.)(sec)(^oR)	Coolant velocity, u_l, ft/sec	$\Psi_{ac} = (H_{out} - H_{in}) \times F\theta/IA_2\eta$, Btu/lb	$\Psi_{max} = (H_{max} - H_{in}) \times F\theta/IA_2\eta$, Btu/lb	Cooling utilization ratio, φ
2.338	H_2-O_2	B	2.8185	0.6750	86.04	5.60	204.4	2.3	9.95	0.00321	0.00922	0.000742	227	713.8	3711.2	0.192
23.38		C	28.1852	6.7504	537.2	4.38	105.6	.7	7.91	.00255	.00692	.000731	161	348.6	3711.2	.0939
233.8		A	281.852	67.504	4408.4	3.51	68.4	.7	6.29	.00203	.00527	.000723	109	229.2	3711.2	.0618
2338		D	2818.52	675.04	34197.1	2.60	38.3	.5	4.99	.00161	.00404	.000716	69	131.7	3711.2	.0355
2.338	H_2-F_2	B	2.6889	.4041	86.04	6.96	403.0	25.9	12.35	.00276	.0129	.000754	495	1481.9	3711.2	.399
23.38		C	26.889	4.041	537.2	5.44	206.8	3.4	9.81	.00219	.00936	.000741	371	723.2	3711.2	.195
233.8		A	268.89	40.41	4408.4	4.36	142.2	2.7	7.80	.00174	.00699	.000731	253	475.6	3711.2	.128
2338		D	2688.9	404.1	34197.1	3.20	81.6	1.7	6.19	.00138	.00527	.000723	152	270.8	3711.2	.0730
2.338	JP4-O_2	B	3.8343	1.1729	86.04	2.46	321.8	377.0	2.95	.00342	.00780	.000854	39	180.5	245.6	.735
23.38		C	38.343	11.729	537.2	2.17	188.5	96.1	2.81	.00263	.00725	.000855	44	99.39	245.6	.405
233.8		A	383.43	117.29	4408.4	1.91	139.8	45.7	2.63	.00199	.00667	.000856	49	71.79	245.6	.292
2338		D	3834.3	1172.9	34197.1	1.59	92.3	28.3	2.42	.00148	.00597	.000858	49	46.36	245.6	.189
2.338	N_2H_4-F_2	B	3.1692	1.0113	86.04	7.69	754.1	-----	13.15	.00203	.0521	.000800	62	654.3	338.8	1.931
23.38		C	31.692	10.113	537.2	6.07	401.0	986.0	10.50	.00161	.0355	.000812	52	322.4	338.8	.952
233.8		A	316.92	101.13	4408.4	4.89	273.0	59.0	8.37	.00127	.0256	.000823	45	213.2	338.8	.629
2338		D	3169.2	1011.3	34197.1	3.66	161.9	15.0	6.67	.00101	.0186	.000832	36	123.8	338.8	.365
2.338	NH_3-F_2	B	3.2029	.7985	86.04	7.84	514.3	-----	13.61	.00206	.176	.000988	153	844.8	184.5	4.579
23.38		C	32.029	7.985	537.2	6.16	320.2	-----	10.86	.00163	.0960	.00101	115	414.4	184.5	2.246
233.8		A	320.29	79.85	4408.4	4.95	231.8	905.7	8.66	.00129	.0625	.00103	96	273.3	184.5	1.481
2338		D	3202.9	798.5	34197.1	3.67	142.6	58.1	6.89	.00102	.0414	.00104	77	157.2	184.5	.852
2.338	NH_3-F_2[a]	B	3.2029	.7985	86.04	5.44	407.0	-----	7.35	.00371	.0540	.00104	54	586.2	184.5	3.177
23.38		C	32.029	7.985	537.2	4.55	253.9	-----	6.71	.00279	.0437	.00104	56	306.1	184.5	1.659
233.8		A	320.29	79.85	4408.4	3.82	185.9	95.4	6.00	.00208	.0357	.00105	57	210.9	184.5	1.143
2338		D	3202.9	798.5	34197.1	2.96	116.9	24.5	5.23	.00154	.0282	.00105	52	126.8	184.5	.687

[a]With ceramic lining.

TABLE II. - SEVERAL PERTINENT CALCULATED QUANTITIES FOR ENGINES OF FIGURE 7

Variable	Over-all engine values								Conditions at throat					Cooling potential		
Performance efficiency, η	Propellant combination	Engine geometry (fig. 4)	Propellant flow rate, w_p, lb/sec	Coolant flow rate, w_l, lb/sec	Cooled surface area, S, sq in.	Average heat flux, q_m, Btu/(sec)(sq in.)	Coolant temperature rise, $T_{out} - T_{in}$, ^oR	Coolant pressure drop, $P_{in} - P_{out}$, lb/sq in.	Heat flux, q, Btu/(sec)(sq in.)	Gas-side heat-transfer coefficient, h_g, Btu/(sq in.)(sec)(^oR)	Coolant-side heat-transfer coefficient, h_l, Btu/(sq in.)(sec)(^oR)	Wall thermal conductivity, k_m, Btu/(in.)(sec)(^oR)	Coolant velocity, u_l, ft/sec	$\Psi_{ac} = (H_{out} - H_{in}) \times F\theta/IA_2\eta$, Btu/lb	$\Psi_{max} = (H_{max} - H_{in}) \times F\theta/IA_2\eta$, Btu/lb	Cooling utilization ratio, φ
1.00	H_2-F_2	A	268.89	40.41	4408.4	4.36	142.2	2.7	7.80	0.00174	0.00699	0.000731	253	475.6	3711.2	0.128
.95		A	283.04	42.54	4408.4	3.71	116.4	1.3	6.62	.00170	.00571	.000725	169	384.5	3711.2	.104
.90		A	298.77	44.90	4408.4	3.13	92.9	.7	5.59	.00167	.00466	.000719	113	307.3	3711.2	.0828
1.00	JP4-O_2	A	383.43	117.29	4408.4	1.91	139.8	45.7	2.63	.00199	.00667	.000856	49	71.79	245.6	.292
.95		A	403.61	123.46	4408.4	1.57	110.3	17.1	2.14	.00148	.00522	.000859	38	56.06	245.6	.228
.90		A	426.03	130.32	4408.4	1.31	88.3	7.8	1.75	.00121	.00415	.000862	29	44.31	245.6	.180
1.00	N_2H_4-F_2	A	316.92	101.13	4408.4	4.89	273.0	59.0	8.37	.00127	.0256	.000823	45	213.2	338.8	.629
.95		A	333.25	106.34	4408.4	4.25	227.6	20.9	6.99	.00119	.0203	.000830	36	176.2	338.8	.520
.90		A	351.77	112.25	4408.4	3.95	201.3	12.0	6.28	.00122	.0178	.000834	31	155.1	338.8	.458

TABLE III. - SEVERAL PERTINENT CALCULATED QUANTITIES FOR ENGINES OF FIGURE 8

Variable	Over-all engine values								Conditions at throat					Cooling potential		
Percent fuel by weight	Propellant combination	Engine geometry (fig. 4)	Propellant flow rate, w_p, lb/sec	Coolant flow rate, w_l, lb/sec	Cooled surface area, S, sq in.	Average heat flux, q_m, Btu/(sec)(sq in.)	Coolant temperature rise, $T_{out} - T_{in}$, ^oR	Coolant pressure drop, $P_{in} - P_{out}$, lb/sq in.	Heat flux, q, Btu/(sec)(sq in.)	Gas-side heat-transfer coefficient, h_g, Btu/(sq in.)(sec)(^oR)	Coolant-side heat-transfer coefficient, h_l, Btu/(sq in.)(sec)(^oR)	Wall thermal conductivity, k_m, Btu/(in.)(sec)(^oR)	Coolant velocity, u_l, ft/sec	$\psi_{ac} = (H_{out} - H_{in}) \times F\theta/IA_2\eta$, Btu/lb	$\psi_{max} = (H_{max} - H_{in}) \times F\theta/IA_2\eta$, Btu/lb	Cooling utilization ratio, φ
23.95	H_2-O_2	A	281.852	67.504	4408.4	3.51	68.4	0.7	6.29	0.00203	0.00527	0.000723	109	229.2	3711.2	0.618
29.15	JP4-O_2	A	384.78	112.16	4408.4	2.11	159.5	77.4	2.85	.00260	.00741	.000855	54	82.93	245.6	.338
30.59	↓	A	383.43	117.29	4408.4	1.91	139.8	45.7	2.63	.00199	.00667	.000856	49	71.79	245.6	.292
34.59	↓	A	387.49	134.03	4408.4	1.52	99.4	13.8	2.06	.00125	.00496	.000860	36	49.99	245.6	.204
5.038	H_2-F_2	A	293.585	14.791	4408.4	6.79	553.9	119.5	12.21	.00181	.0149	.000753	1077	2023.7	3711.2	.545
7.045	↓	A	282.20	19.881	4408.4	6.56	395.0	45.7	12.10	.00191	.0137	.000752	955	1454.6	3711.2	.392
9.593	↓	A	276.47	26.521	4408.4	5.39	250.1	10.1	9.63	.00171	.00953	.000740	522	895.9	3711.2	.241
15.03	↓	A	268.89	40.410	4408.4	4.36	142.2	2.7	7.80	.00174	.00699	.000731	253	475.6	3711.2	.128
20.97	↓	A	269.98	56.615	4408.4	3.59	84.0	.9	6.44	.00191	.00545	.000724	127	279.5	3711.2	.0753
31.91	N_2H_4-F_2	A	316.59	101.02	4408.4	4.89	273.0	59.0	8.37	.00127	.0256	.000823	45	213.4	338.8	.630
34.52	↓	A	316.28	109.18	4408.4	5.05	261.4	61.8	9.05	.00141	.0268	.000819	48	203.9	338.8	.602
37.59	↓	A	317.75	119.44	4408.4	4.79	228.3	35.4	8.43	.00136	.0238	.000822	43	176.8	338.8	.522

TABLE IV. - SEVERAL PERTINENT CALCULATED QUANTITIES FOR ENGINES OF FIGURE 9

Variable	Over-all engine values								Conditions at throat					Cooling potential		
Nozzle expansion ratio, A_3/A_2	Propellant combination	Engine geometry (fig. 4)	Propellant flow rate, w_p, lb/sec	Coolant flow rate, w_l, lb/sec	Cooled surface area, S, sq in.	Average heat flux, q_m, Btu/(sec)(sq in.)	Coolant temperature rise, $T_{out} - T_{in}$, ^oR	Coolant pressure drop, $P_{in} - P_{out}$, lb/sq in.	Heat flux, q, Btu/(sec)(sq in.)	Gas-side heat-transfer coefficient, h_g, Btu/(sq in.)(sec)(^oR)	Coolant-side heat-transfer coefficient, h_l, Btu/(sq in.)(sec)(^oR)	Wall thermal conductivity, k_m, Btu/(in.)(sec)(^oR)	Coolant velocity, u_l, ft/sec	$\psi_{ac} = (H_{out} - H_{in}) \times F\theta/IA_2\eta$, Btu/lb	$\psi_{max} = (H_{max} - H_{in}) \times F\theta/IA_2\eta$, Btu/lb	Cooling utilization ratio, φ
3.8	H_2-F_2	A	268.89	40.41	4408.4	4.36	142.2	2.7	7.80	0.00174	0.00699	0.000731	253	475.6	3711.2	0.128
25	↓	K	268.89	40.41	23562.6	1.24	207.2	5.1	7.80	.00174	.00749	.000731	440	723.0	3711.2	.195
50	↓	L	268.89	40.41	44930.8	.70	220.7	5.6	7.80	.00174	.00759	.000731	477	778.3	3711.2	.210
3.8	JP4-O_2	A	383.43	117.29	4408.4	1.91	139.8	45.7	2.63	.00199	.00667	.000856	49	71.79	245.6	.292
25	↓	K	383.43	117.29	23562.6	.74	270.0	175.9	2.63	.00199	.0102	.000856	73	148.7	245.6	.605
50	↓	L	383.43	117.29	44930.8	.46	313.2	353.3	2.63	.00199	.0124	.000856	90	176.2	245.6	.717
3.8	N_2H_4-F_2	A	316.59	101.02	4408.4	4.89	273.0	59.0	8.37	.00127	.0256	.000823	45	213.4	338.8	.630
25	↓	K	316.59	101.02	23562.6	1.78	506.3	-----	8.37	.00127	.104	.000823	193	415.2	338.8	1.226
50	↓	L	316.59	101.02	44930.8	1.17	616.5	-----	8.35	.00128	-------	.000809	---	520.4	338.8	1.536

TABLE V. - SEVERAL PERTINENT CALCULATED QUANTITIES FOR ENGINES OF FIGURE 10

Variable	Over-all engine values								Conditions at throat					Cooling potential		
Combustion-chamber pressure, p_1, lb/sq in. abs	Propellant combination	Engine geometry (fig. 4)	Propellant flow rate, w_p, lb/sec	Coolant flow rate, w_l, lb/sec	Cooled surface area, S, sq in.	Average heat flux, q_m, Btu/(sec)(sq in.)	Coolant temperature rise, $T_{out} - T_{in}$, $^\circ R$	Coolant pressure drop, $p_{in} - p_{out}$, lb/sq in.	Heat flux, q, Btu/(sec)(sq in.)	Gas-side heat-transfer coefficient, h_g, Btu/(sq in.)(sec)($^\circ R$)	Coolant-side heat-transfer coefficient, h_l, Btu/(sq in.)(sec)($^\circ R$)	Wall thermal conductivity, k_m, Btu/(in.)(sec)($^\circ R$)	Coolant velocity, u_l, ft/sec	$\psi_{ac} = (H_{out} - H_{in}) \times F\theta/IA_2\eta$, Btu/lb	$\psi_{max} = (H_{max} - H_{in}) \times F\theta/IA_2\eta$, Btu/lb	Cooling utilization ratio, φ
60	H_2-F_2	E	55.047	8.272	4408.4	1.06	185.3	0.4	1.89	0.000446	0.00152	0.000699	255	564.9	3627.1	0.156
60		F	269.40	40.48	16630.3	.92	133.1	.3	1.75	.000392	.00140	.000698	266	378.0	3627.1	.104
300		A	268.89	40.41	4408.4	4.36	142.2	2.7	7.80	.00174	.00699	.000731	253	475.6	3711.2	.128
600		J	269.15	40.45	2566.1	8.23	144.0	9.3	14.73	.00321	.0154	.000765	293	522.1	3758.5	.139
600		I	535.05	80.40	4408.4	7.65	116.3	6.8	13.78	.00301	.0140	.000761	268	419.5	3758.5	.112
60	JP4-O_2	E	78.32	22.83	4408.4	.87	302.1	46.0	1.47	.000546	.00477	.000864	26	168.0	245.6	.684
60		F	383.29	111.73	16630.3	.71	199.1	7.6	1.27	.000427	.00386	.000865	24	105.7	245.6	.430
300		A	384.78	112.16	4408.4	2.11	159.5	77.4	2.85	.00260	.00741	.000855	54	82.93	245.6	.338
600		J	384.17	111.99	2566.1	2.70	121.2	90.9	3.23	.00454	.00784	.000852	59	61.87	245.6	.252
600		I	763.70	222.62	4408.4	2.60	101.9	56.5	3.20	.00422	.00774	.000853	62	51.49	245.6	.210
150	N_2H_4-F_2	G	159.64	55.107	4408.4	2.84	289.8	18.4	5.10	.000810	.0158	.000841	25	227.2	338.8	.671
150		H	321.23	110.89	7678.1	2.53	226.3	6.3	4.75	.000754	.0141	.000843	23	175.2	338.8	.517
300		A	316.28	109.18	4408.4	5.05	261.4	61.8	9.05	.00141	.0268	.000819	48	203.9	338.8	.602
600		J	315.50	108.91	2566.1	9.24	278.2	377.2	16.18	.00250	.0469	.000789	90	217.7	338.8	.643
600		I	627.19	216.51	4408.4	8.62	226.6	172.0	15.15	.00233	.0427	.000793	87	175.5	338.8	.518

TABLE VI. - SEVERAL PERTINENT CALCULATED QUANTITIES FOR ENGINES OF FIGURE 11

Variable	Over-all engine values								Conditions at throat					Cooling potential		
Engine contraction ratio, A_1/A_2	Propellant combination	Engine geometry (fig. 4)	Propellant flow rate, w_p, lb/sec	Coolant flow rate, w_l, lb/sec	Cooled surface area, S, sq in.	Average heat flux, q_m, Btu/(sec)(sq in.)	Coolant temperature rise, $T_{out} - T_{in}$, $^\circ R$	Coolant pressure drop, $p_{in} - p_{out}$, lb/sq in.	Heat flux, q, Btu/(sec)(sq in.)	Gas-side heat-transfer coefficient, h_g, Btu/(sq in.)(sec)($^\circ R$)	Coolant-side heat-transfer coefficient, h_l, Btu/(sq in.)(sec)($^\circ R$)	Wall thermal conductivity, k_m, Btu/(in.)(sec)($^\circ R$)	Coolant velocity, u_l, ft/sec	$\psi_{ac} = (H_{out} - H_{in}) \times F\theta/IA_2\eta$, Btu/lb	$\psi_{max} = (H_{max} - H_{in}) \times F\theta/IA_2\eta$, Btu/lb	Cooling utilization ratio, φ
1.5	H_2-F_2	M	268.89	40.41	4246.8	4.63	145.3	3.4	7.80	0.00174	0.00699	0.000731	252	486.6	3711.2	0.131
2		A	268.89	40.41	4408.4	4.36	142.2	2.7	7.80	.00174	.00699	.000731	253	475.6	3711.2	.128
3		N	268.89	40.41	4707.8	4.02	140.4	2.3	7.80	.00174	.00699	.000731	253	468.3	3711.2	.126
1.5	JP4-O_2	M	383.43	117.29	4246.8	1.96	138.4	52.5	2.63	.00199	.00667	.000856	49	70.97	245.6	.289
2		A	383.43	117.29	4408.4	1.91	139.8	45.7	2.63	.00199	.00667	.000856	49	71.79	245.6	.292
3		N	383.43	117.29	4707.8	1.82	142.0	38.7	2.63	.00199	.00667	.000856	49	73.05	245.6	.297
1.5	N_2H_4-F_2	M	316.59	101.02	4246.8	5.20	279.0	91.6	8.37	.00127	.0256	.000823	45	218.6	338.8	.645
2		A	316.59	101.02	4408.4	4.89	273.0	59.0	8.37	.00127	.0256	.000823	45	213.4	338.8	.630
3		N	316.59	101.02	4707.8	4.52	269.5	44.4	8.37	.00127	.0256	.000823	45	210.6	338.8	.622

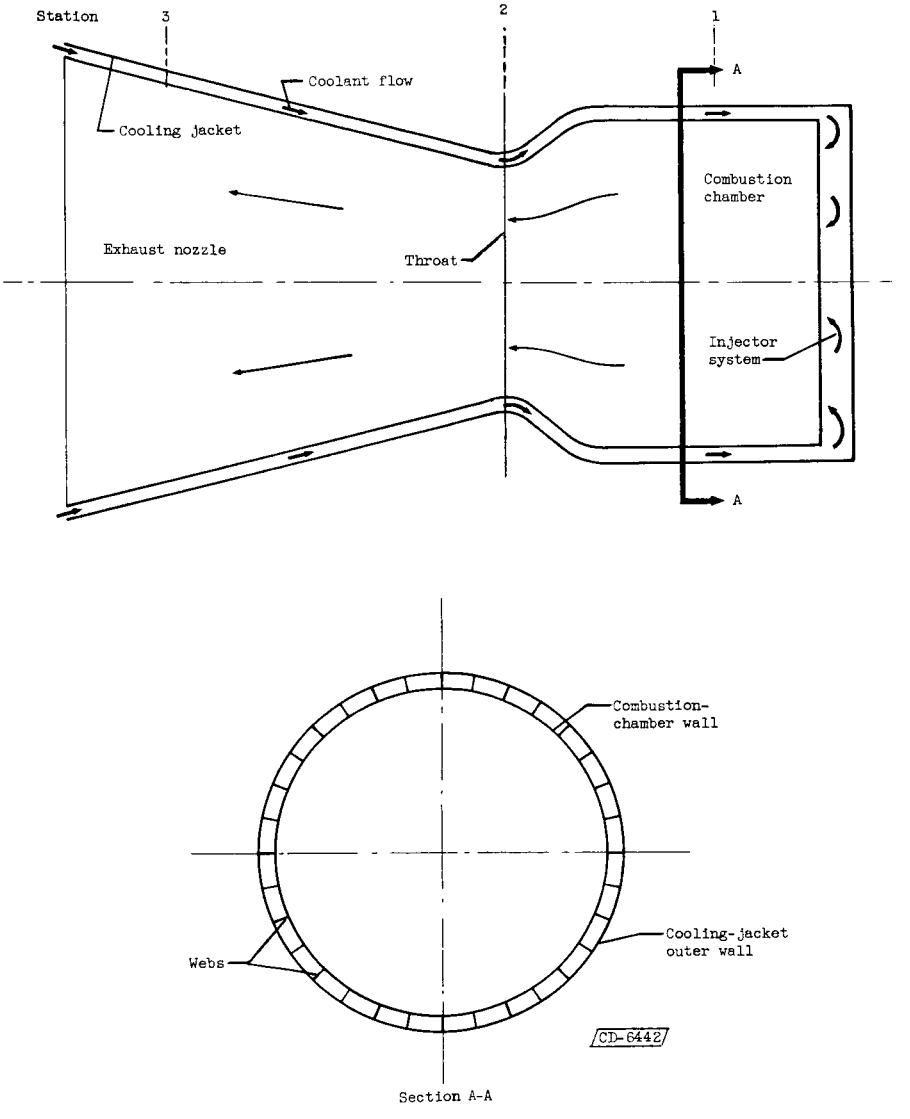

Figure 1. - Schematic diagram of regeneratively cooled rocket engine considered in analysis.

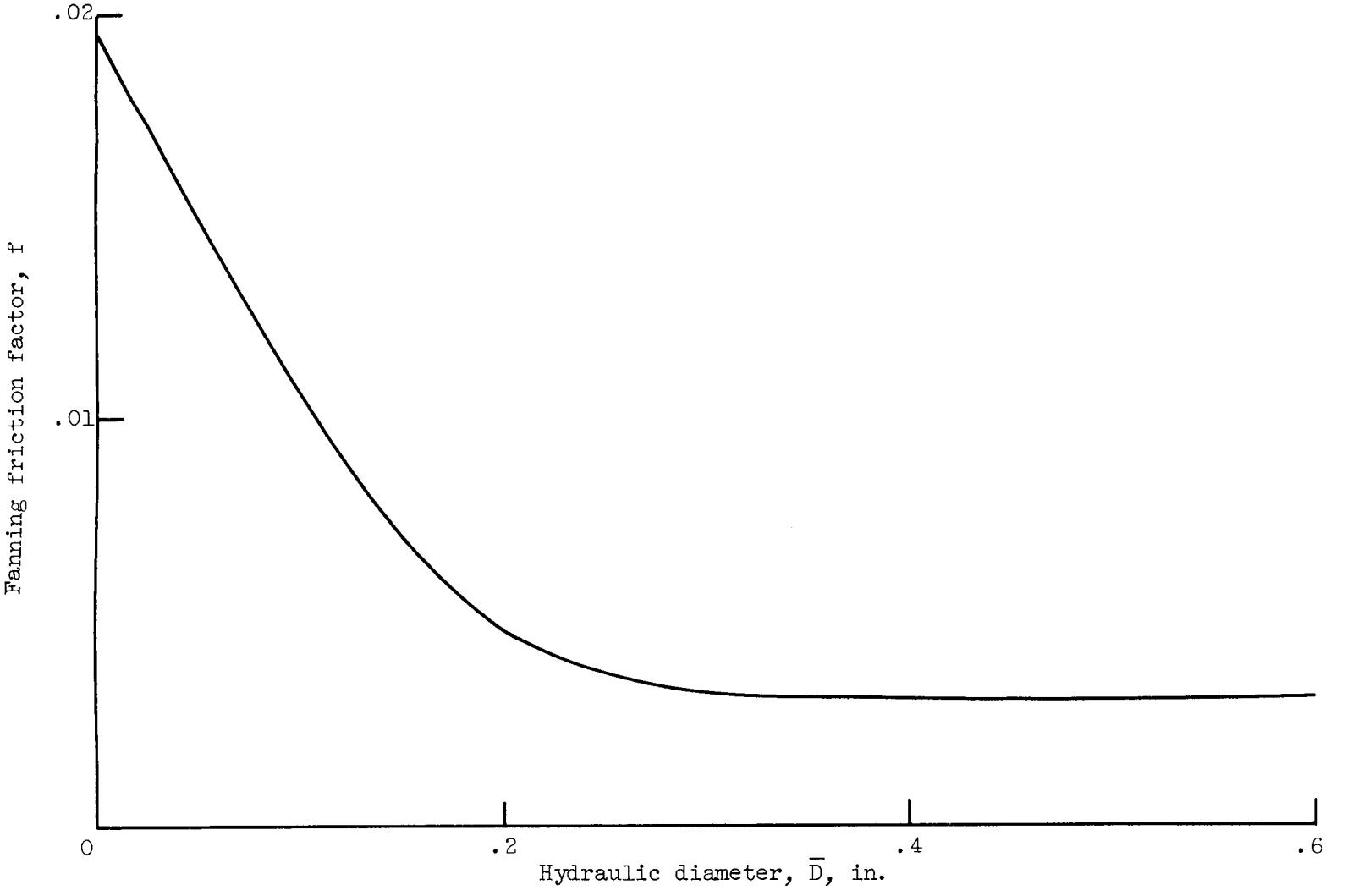

Figure 2. - Relation between Fanning friction factor and hydraulic diameter for Reynolds number of 1,500,000. Curve is for tubing or very clean smooth machined surface (ref. 5).

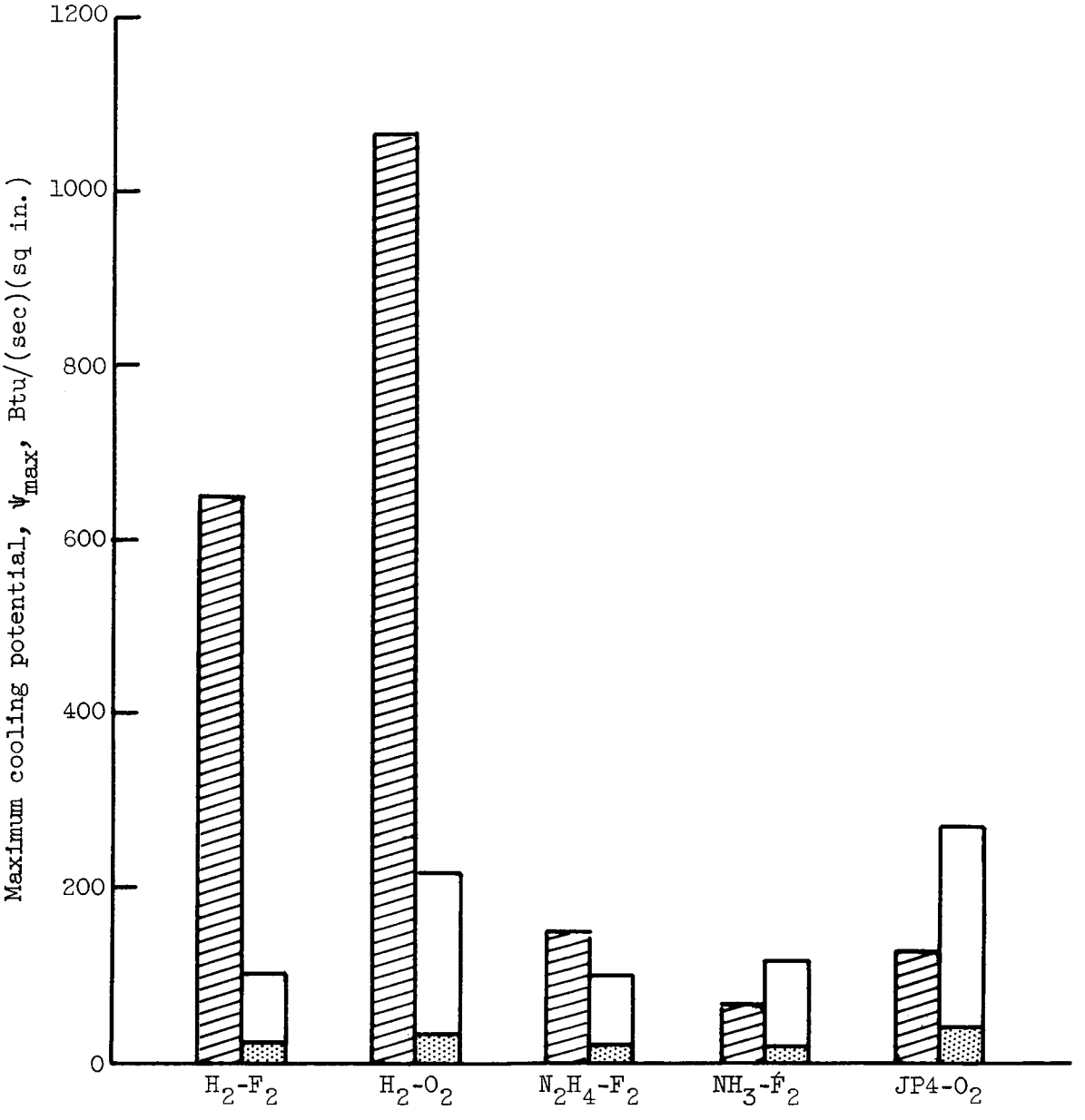

Figure 3. - Comparison of maximum cooling potentials of components of propellant combinations considered in this study. Combustion-chamber pressure, 300 pounds per square inch absolute; contraction ratio, 2; expansion ratio, 3.8; fuel mixture for maximum characteristic velocity.

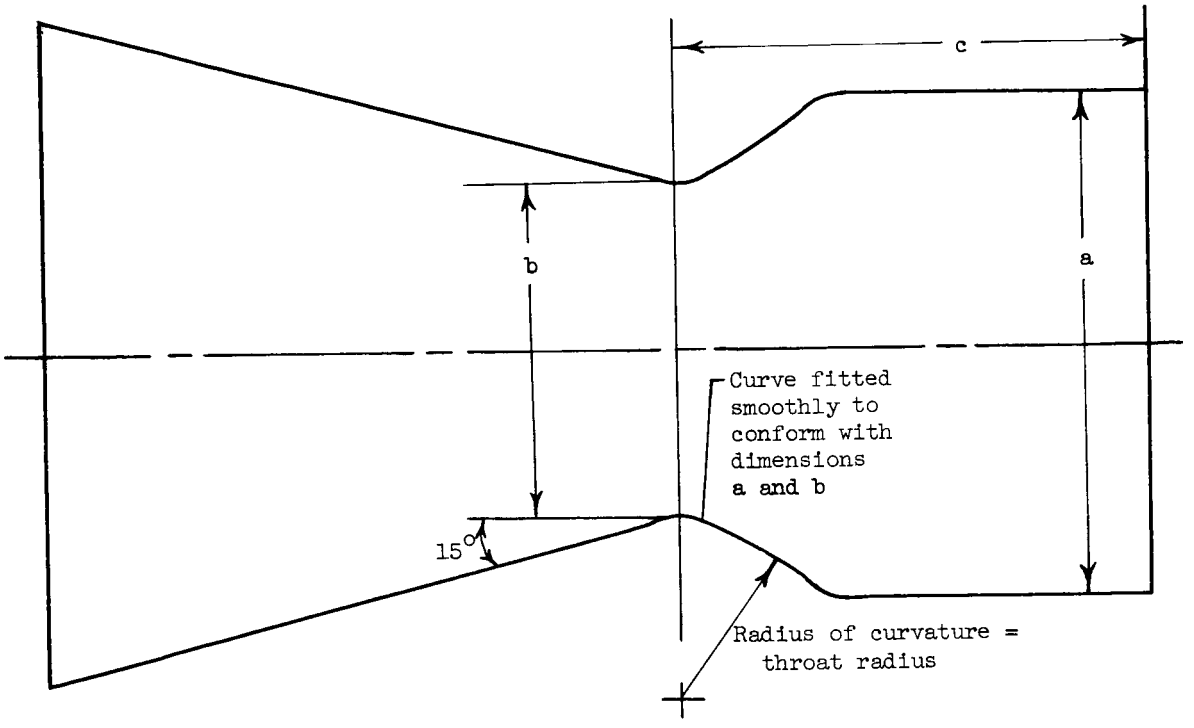

Engine	Throat area, sq in.	Chamber pressure, lb/sq in. abs	Expansion area ratio	Contraction area ratio	Nominal thrust, lb	Number of webs	c, in.
A*	233.8	300	3.8	2	100,000	200	24.0
B	2.338	300	3.8	2	1,000	25	8.0
C	23.38	300	3.8	2	10,000	70	12.0
D	2338.0	300	3.8	2	1,000,000	600	36.0
E	233.8	60	3.8	2	20,000	200	24.0
F	1143.2	60	3.8	2	100,000	200	24.0
G	233.8	150	3.8	2	50,000	200	24.0
H	470.05	150	3.8	2	100,000	200	24.0
I	233.8	600	3.8	2	200,000	200	24.0
J	117.5	600	3.8	2	100,000	200	24.0
K	233.8	300	25	2	124,000	200	24.0
L	233.8	300	50	2	130,000	200	24.0
M	233.8	300	3.8	1.5	100,000	200	24.0
N	233.8	300	3.8	3	100,000	200	24.0

*Reference engine.

Figure 4. - Tabulated combustion-gas-system specifications for rocket engines considered in analysis.

E-150

E-150
CJ-3 back

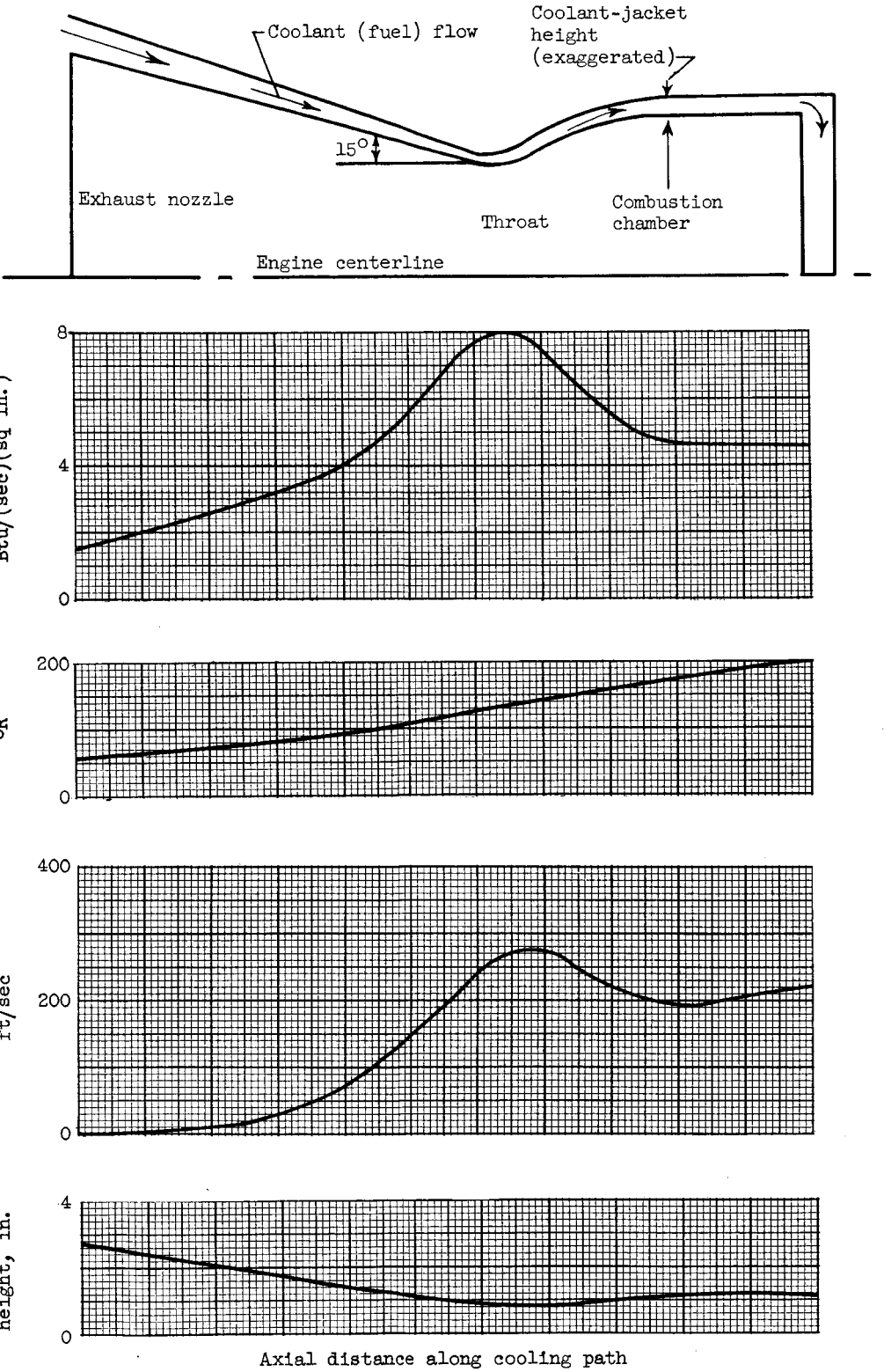

Figure 5. - Typical longitudinal profiles of several important quantities computed for engine A.

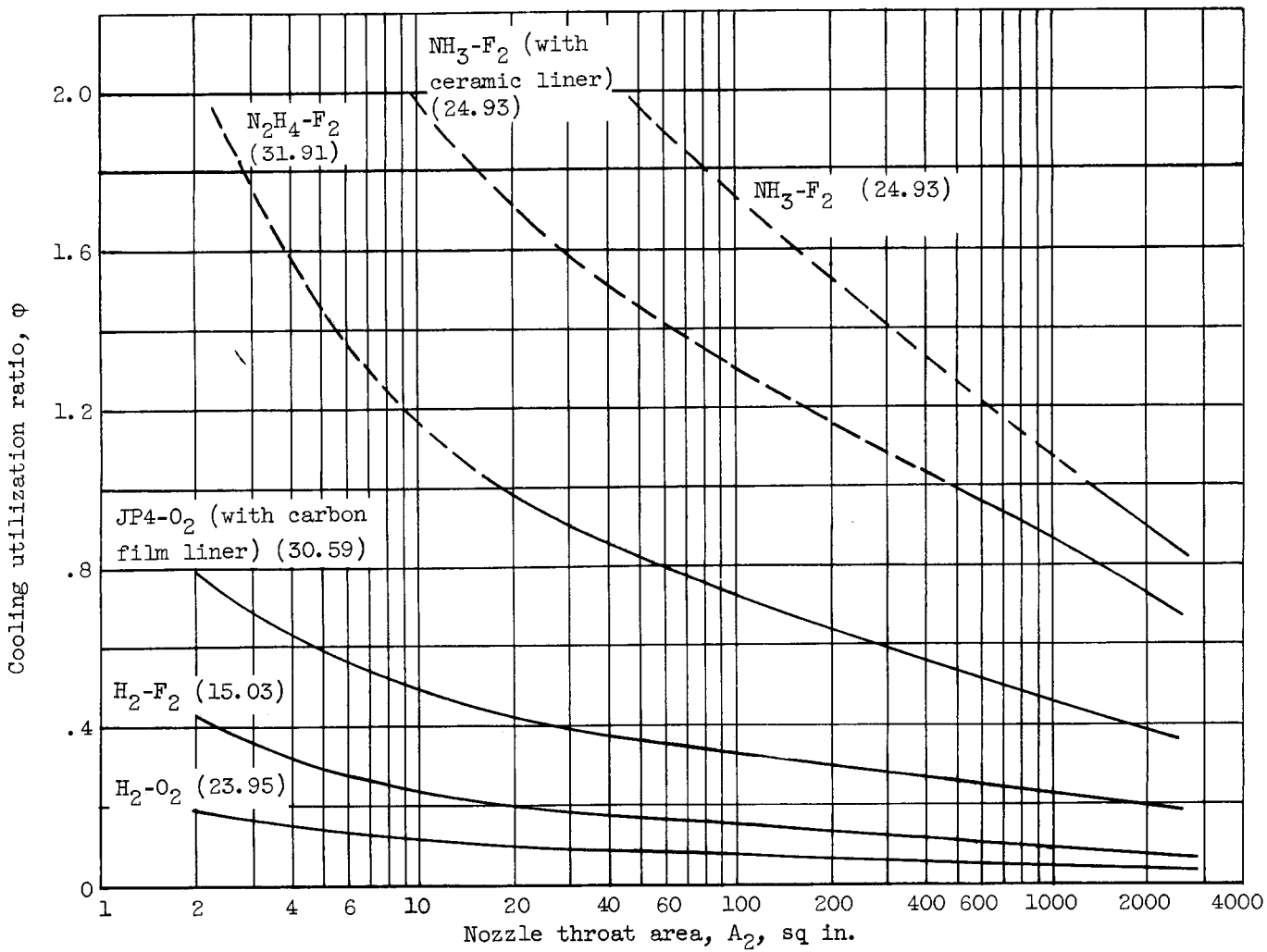

Figure 6. - Relation between cooling utilization ratio and engine size for several propellant combinations. Combustion-chamber pressure, 300 pounds per square inch absolute; contraction ratio, 2; expansion ratio, 3.8; fuel mixture for maximum characteristic velocity. Numbers on curves indicate percent fuel by weight.

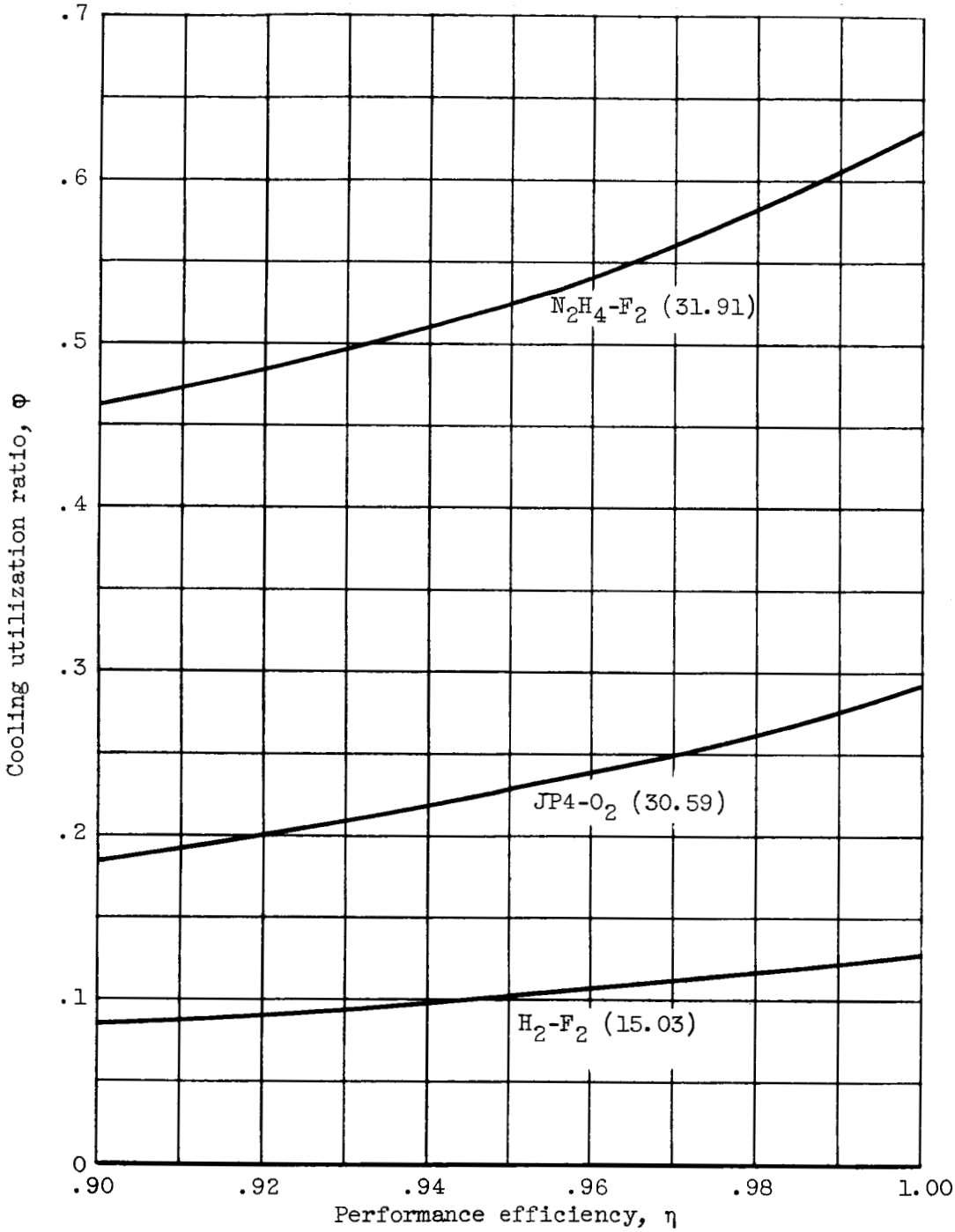

Figure 7. - Relation between cooling utilization ratio and performance efficiency for three propellant combinations. Combustion-chamber pressure, 300 pounds per square inch absolute; nozzle throat area, A_2, 233.8 square inches; contraction ratio, 2; expansion ratio, 3.8. Numbers on curves indicate percent fuel by weight.

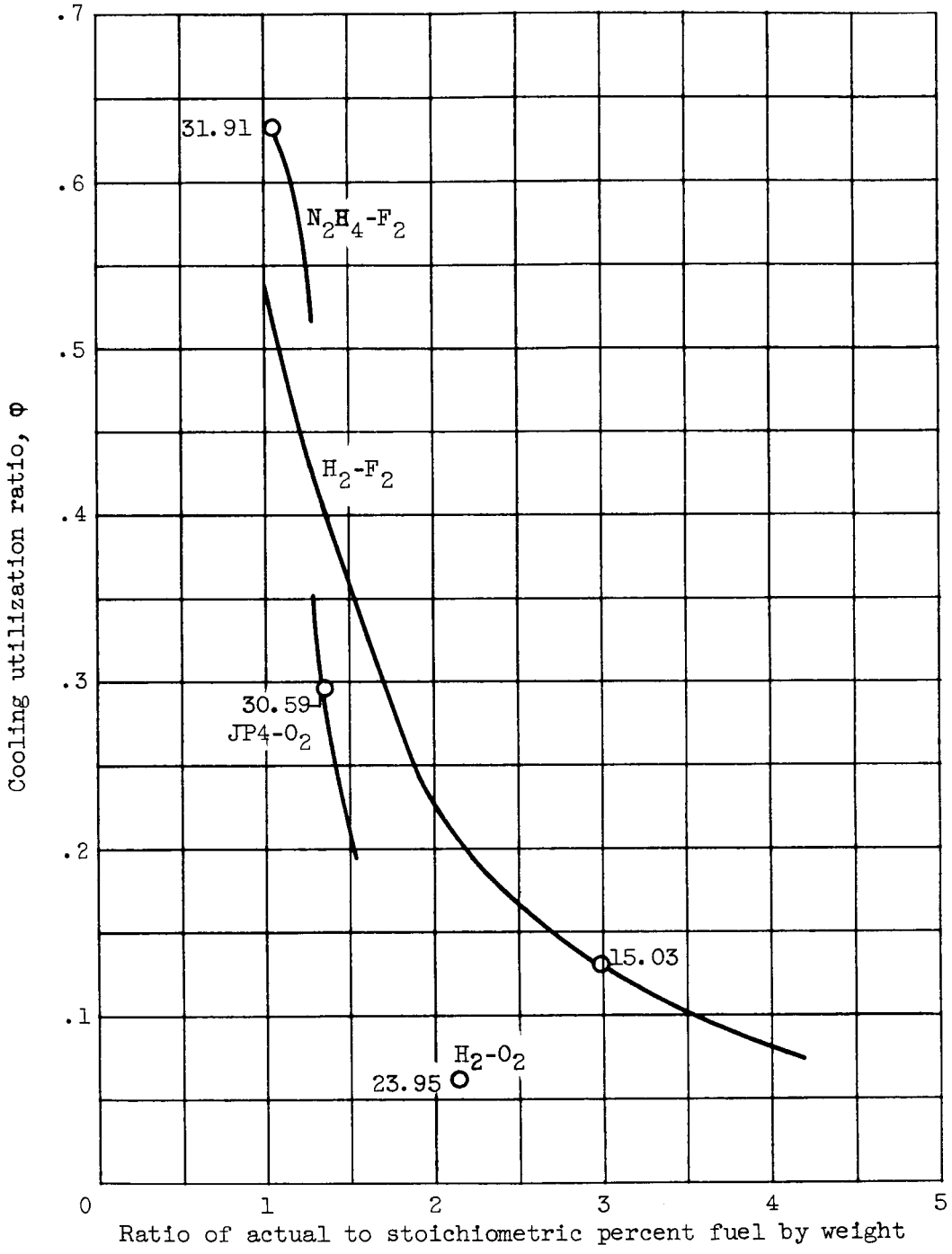

Figure 8. - Relation between cooling utilization ratio and fuel mixture for four propellant combinations. Combustion-chamber pressure, 300 pounds per square inch absolute; nozzle throat area, A_2, 233.8 square inches; contraction ratio, 2; expansion ratio, 3.8. Numbers attached to points on curves indicate percent fuel by weight at that point.

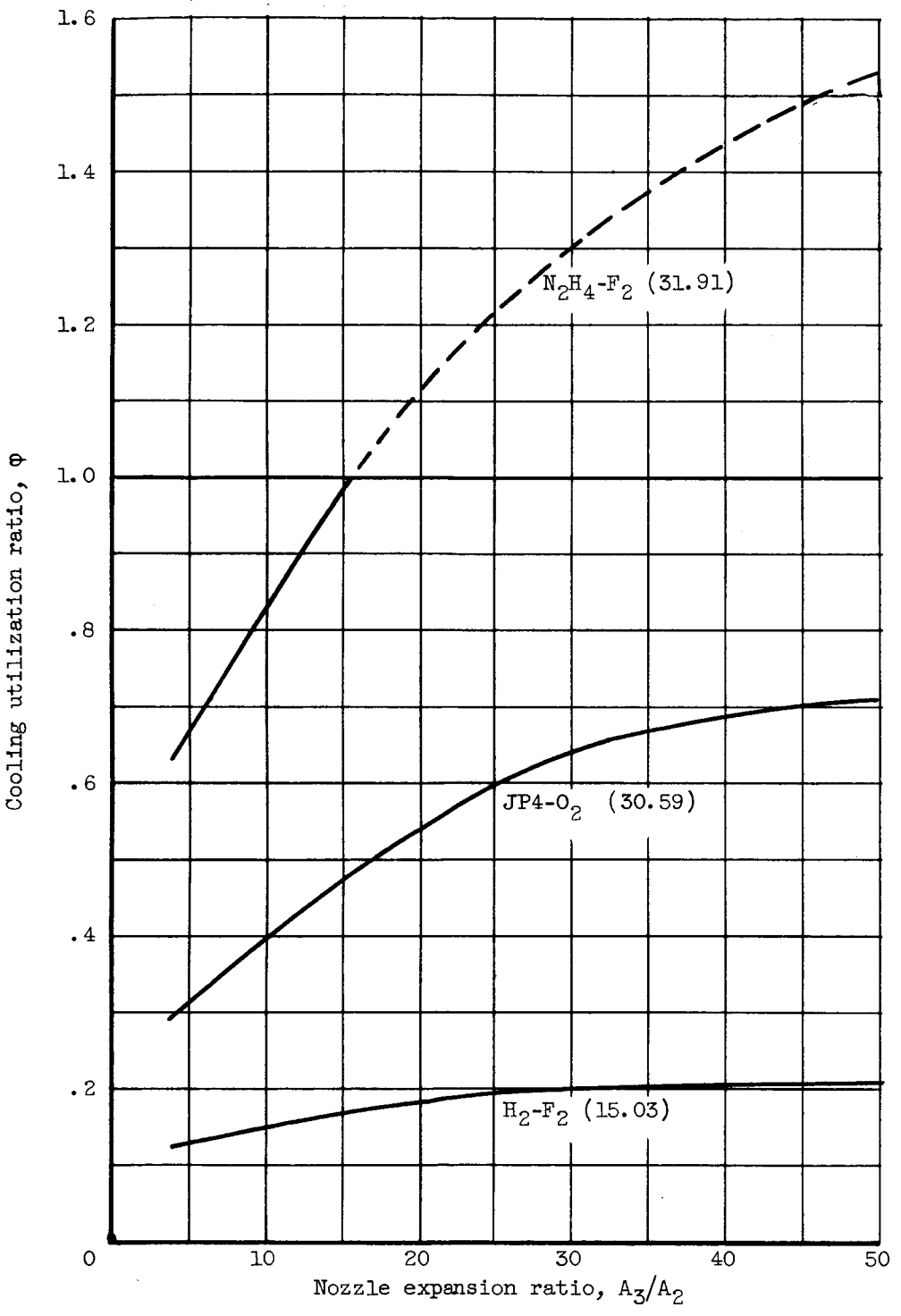

Figure 9. - Relation between cooling utilization ratio and nozzle expansion ratio for three propellant combinations. Combustion-chamber pressure, 300 pounds per square inch absolute; nozzle throat area, A_2, 233.8 square inches; contraction ratio, 2. Numbers on curves indicate percent fuel by weight.

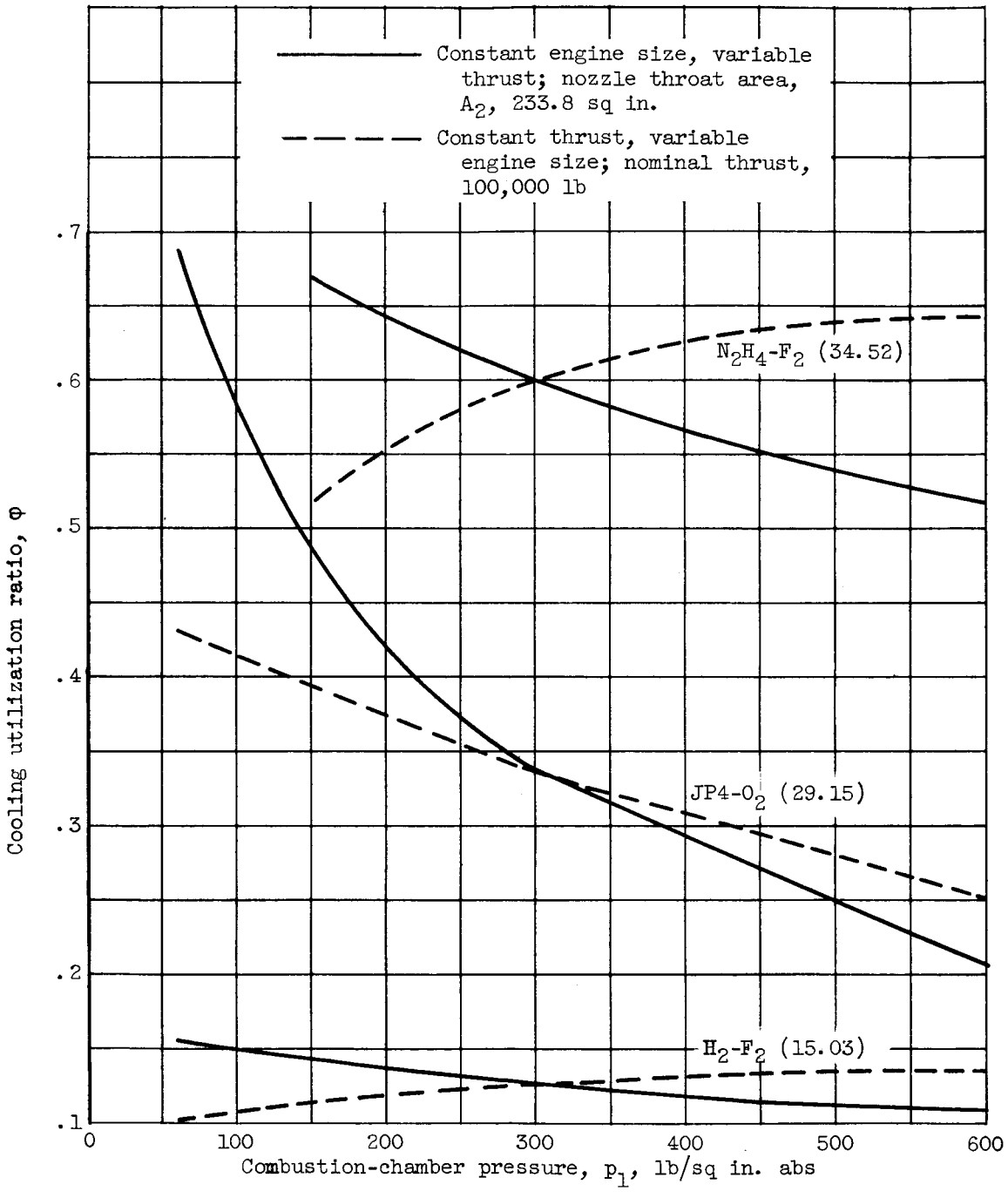

Figure 10. - Relation between combustion-chamber pressure and cooling utilization ratio for three propellant combinations. Engine contraction ratio, 2; expansion ratio, 3.8. Numbers on curves indicate percent fuel by weight.

E-150

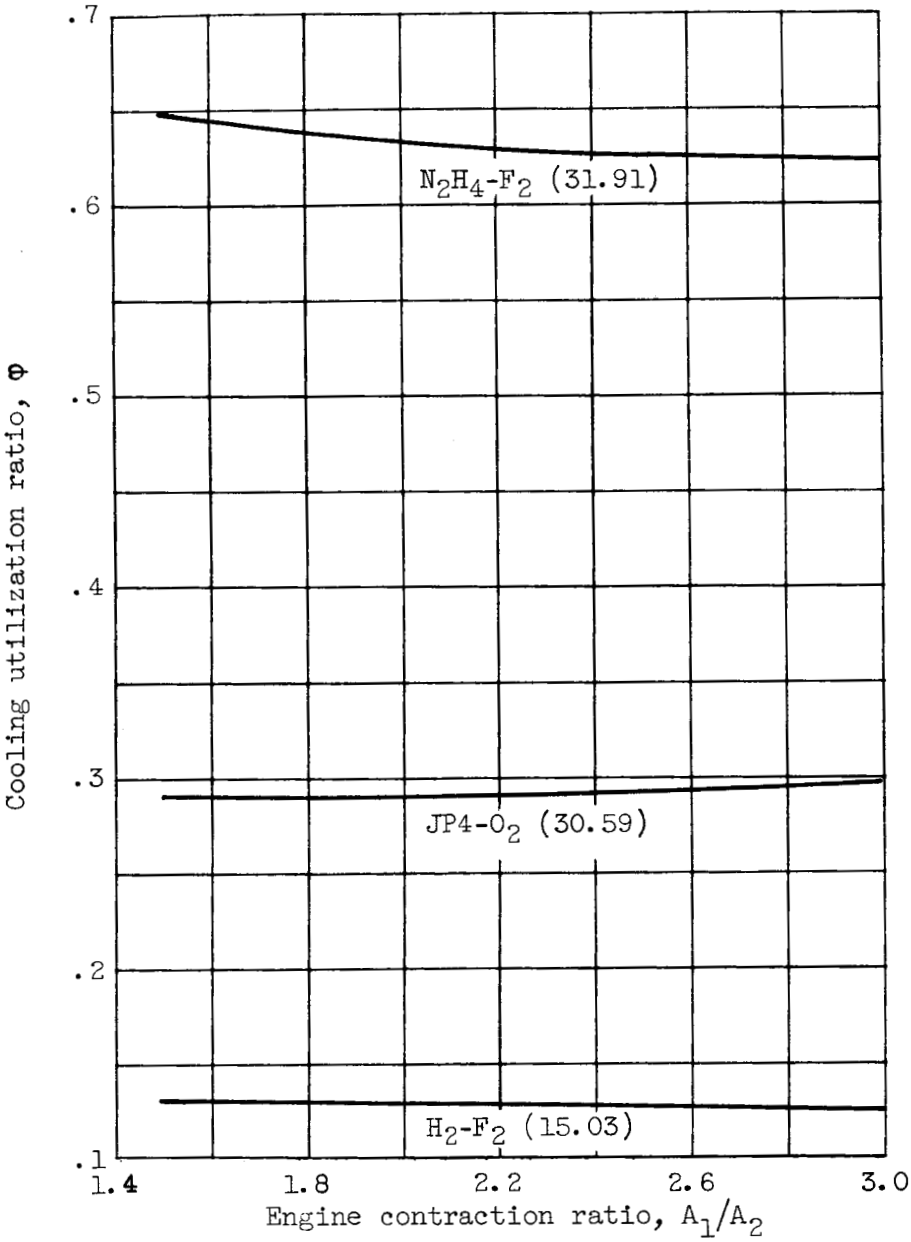

Figure 11. - Relation between cooling utilization ratio and engine contraction ratio for three propellant combinations. Combustion-chamber pressure, 300 pounds per square inch absolute; nozzle throat area, A_2, 233.8 square inches; expansion ratio, 3.8. Numbers on curves indicate percent fuel by weight.

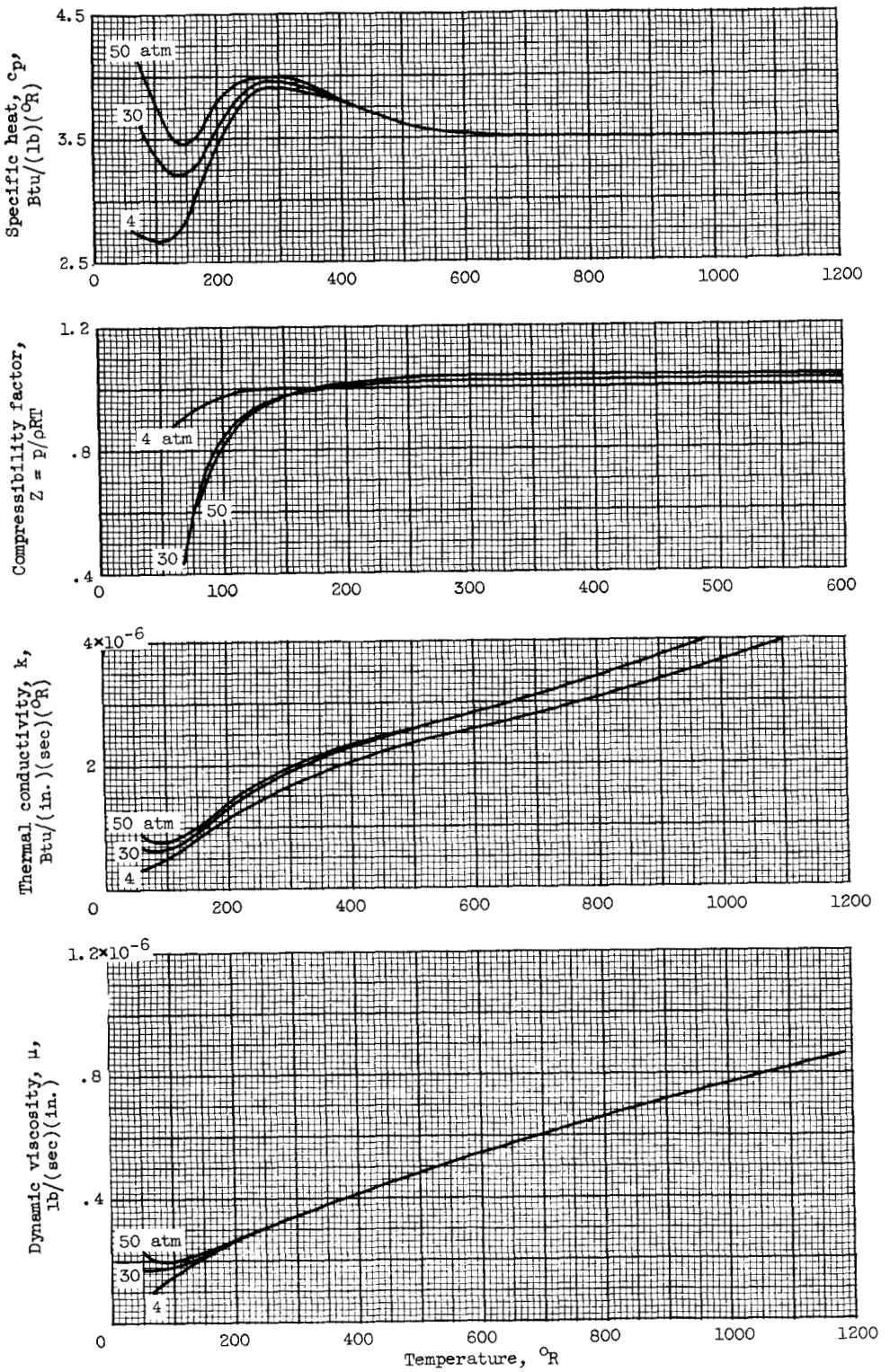

Figure 12. - Some physical properties of gaseous hydrogen as functions of temperature and pressure (refs. 15 and 16).

E-150
CJ-6 back

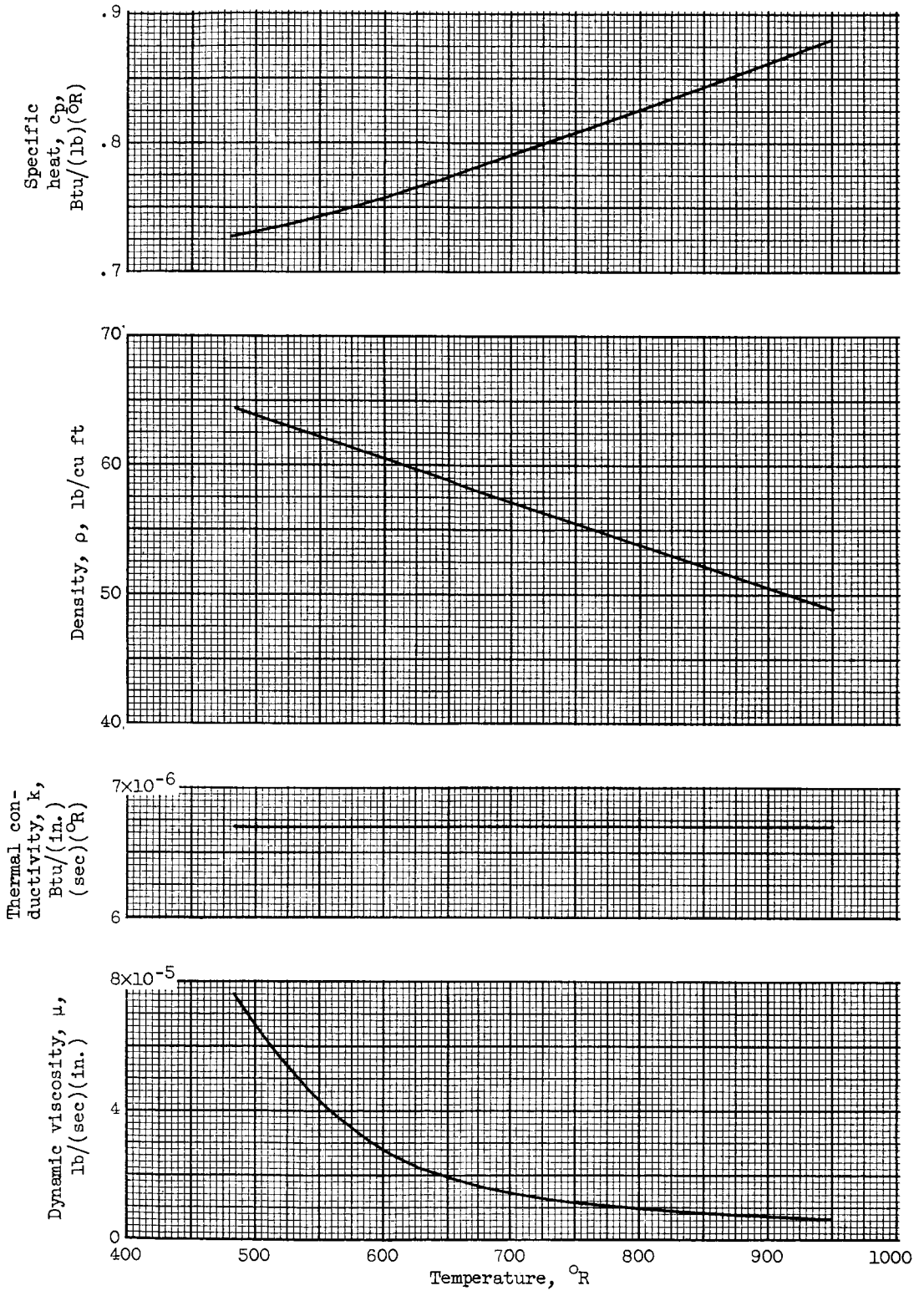

Figure 13. - Some physical properties of liquid hydrazine as functions of temperature.

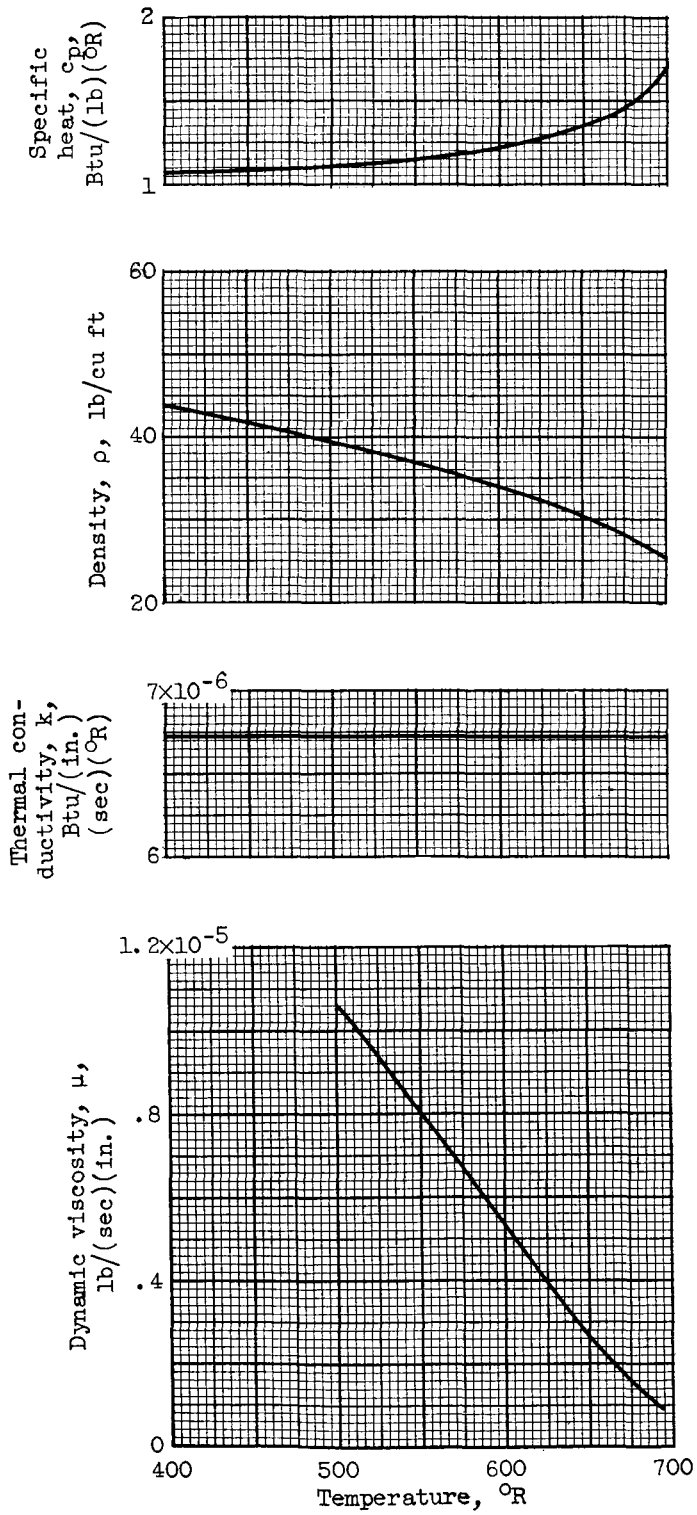

Figure 14. - Some physical properties of liquid ammonia as functions of temperature (ref. 18).

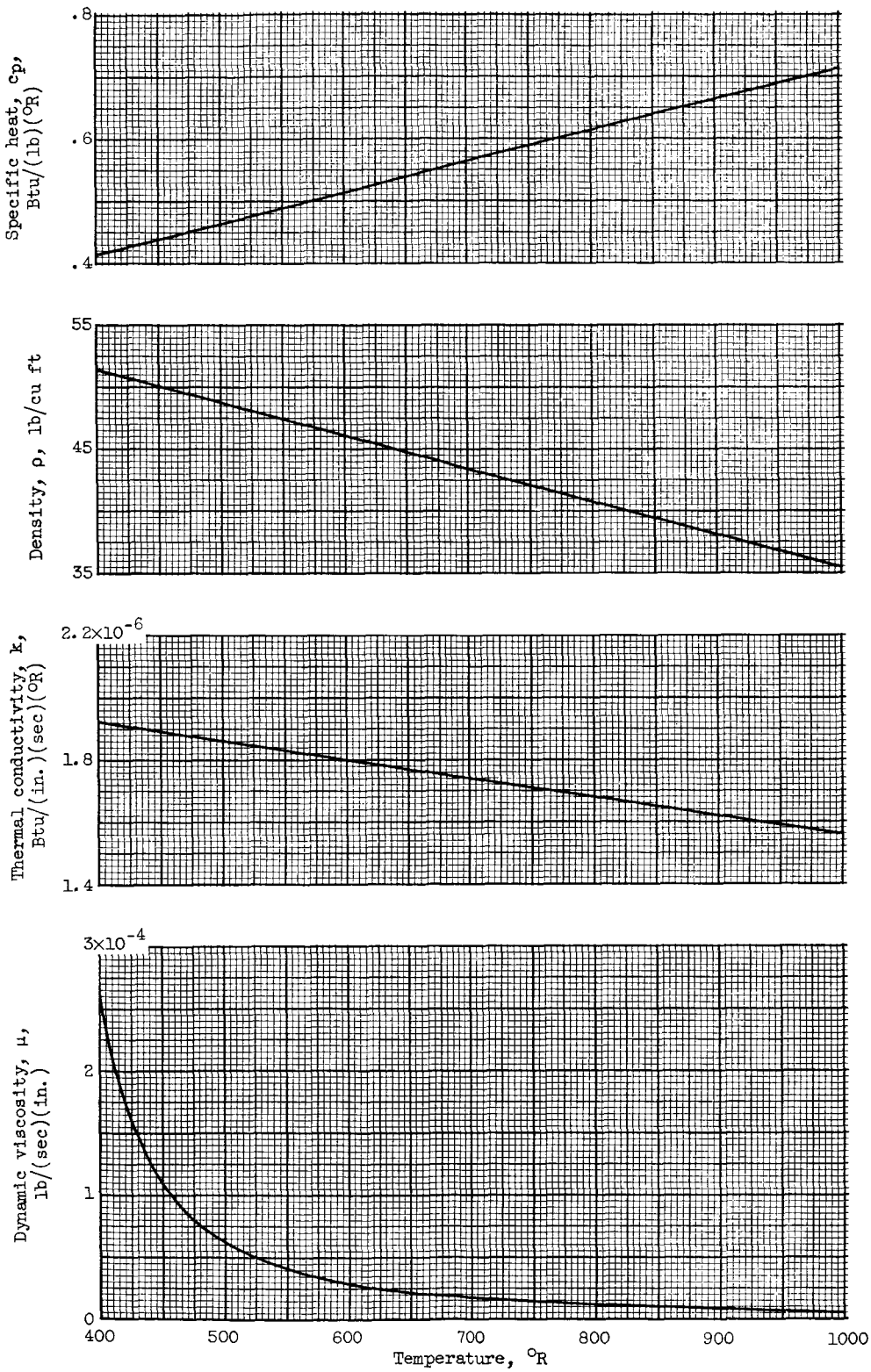

Figure 15. - Some physical properties of liquid JP-4 as functions of temperature (refs. 19 and 20).

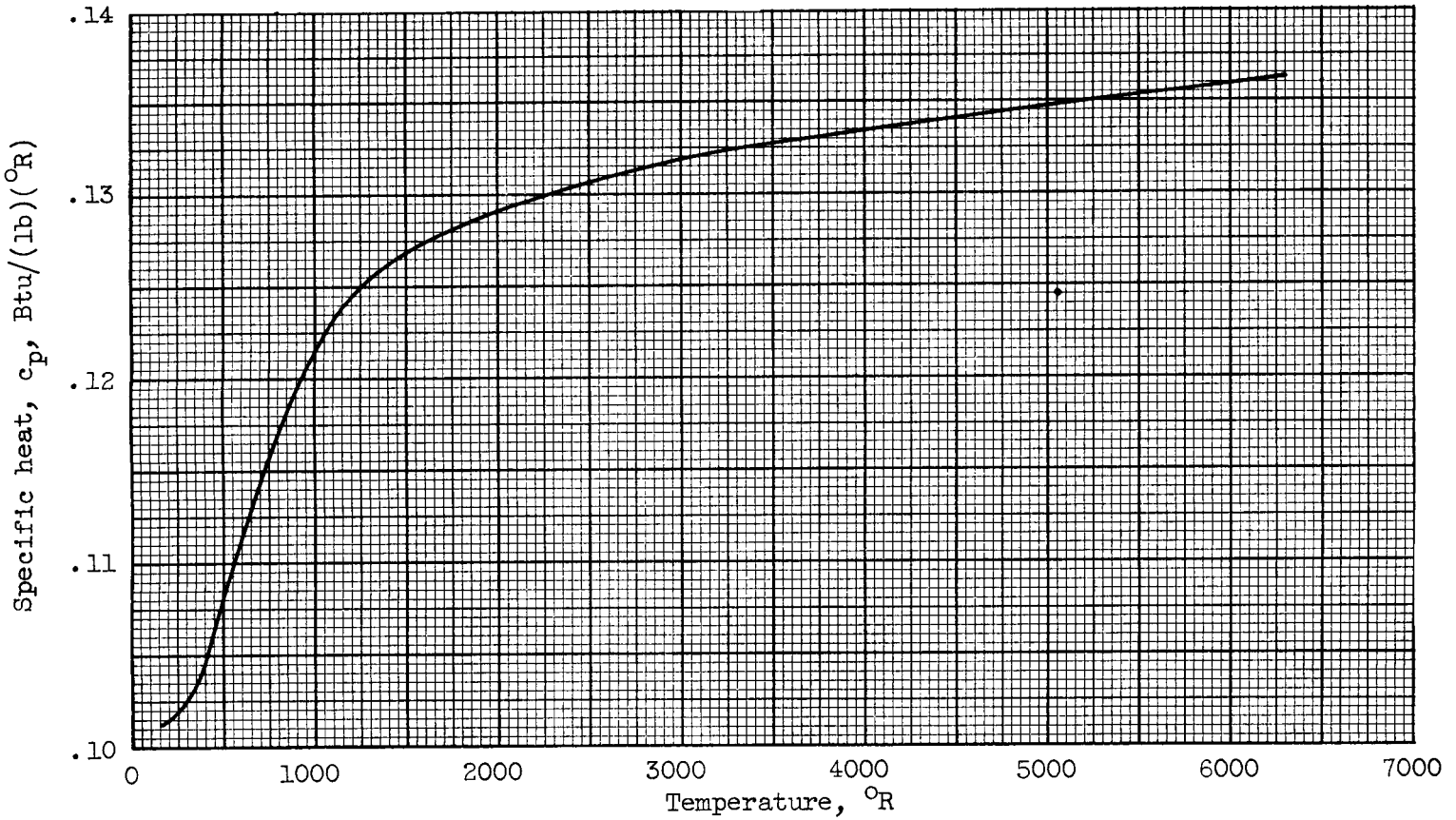

Figure 16. - Specific heat of liquid and gaseous fluorine as function of temperature (refs. 21 to 23).

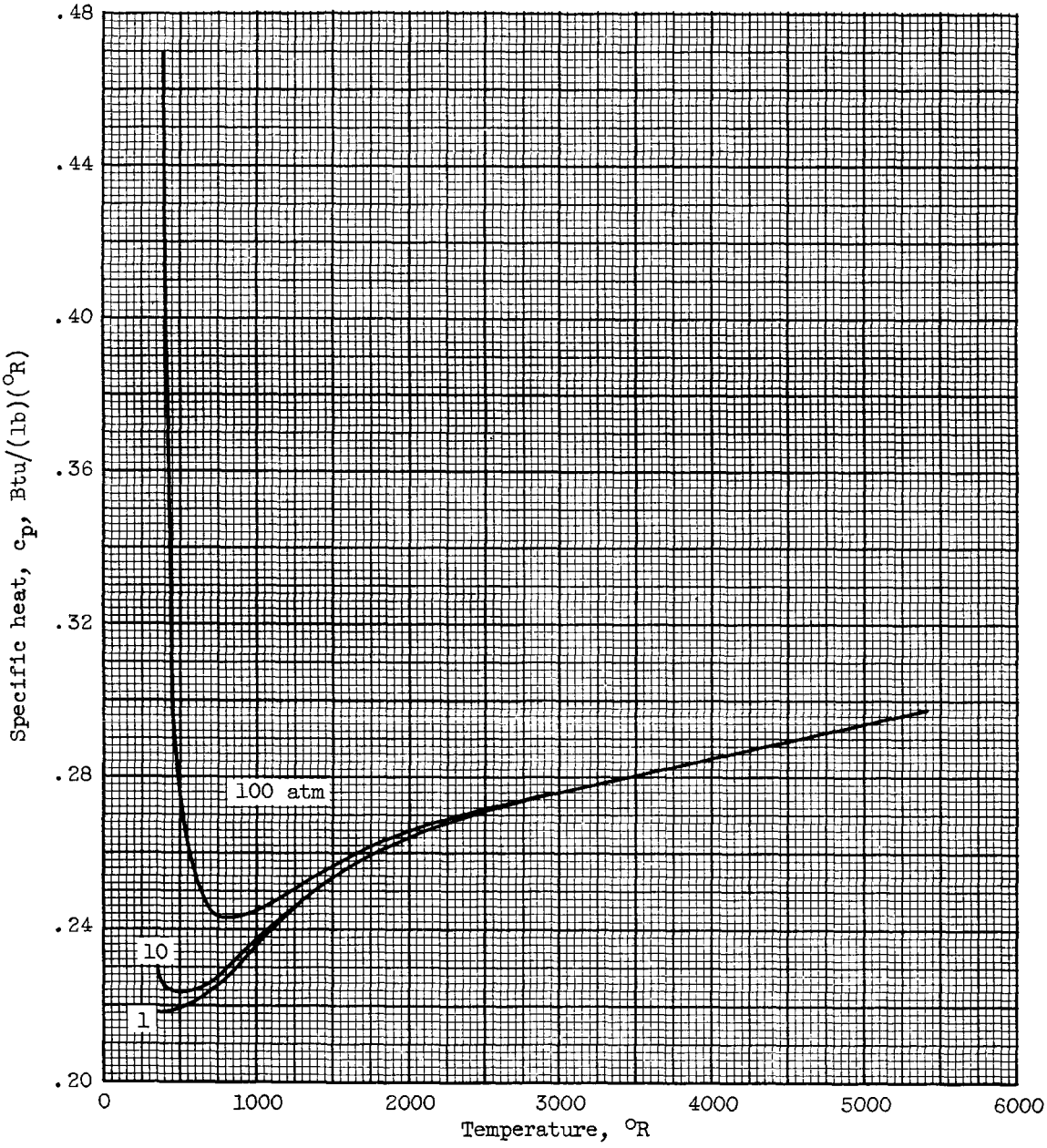

Figure 17. - Specific heat of liquid and gaseous oxygen as function of temperature (refs. 24 and 25).